[AMERICAN JOURNAL OF SCIENCE, VOL. 280, MAY, 1980, P. 421-458]

THE ORIGINS OF POTASSIC MAGMAS: 2. STABILITY OF PHLOGOPITE IN NATURAL SPINEL LHERZOLITE AND IN THE SYSTEM $KAlSiO_4$–MgO–SiO_2–H_2O–CO_2 AT HIGH PRESSURES AND HIGH TEMPERATURES

RICHARD F. WENDLANDT* and DAVID H. EGGLER

Dept. of Geosciences, The Pennsylvania State University, University Park, Pennsylvania 16802

ABSTRACT. Melting relations of phlogopite in portions of the system $KAlSiO_4$–MgO–SiO_2–H_2O–CO_2 have been determined at pressures and temperatures of the upper mantle. Univariant reactions predict the melting behavior of a phlogopite peridotite and illustrate the prominent role of phlogopite in the genesis of potassium-rich basanites, carbonatites, and kimberlites.

The presence of small total volatile contents in mantle peridotite will promote univariant melting behavior in which CO_2–H_2O vapor compositions are buffered, for a given pressure, by phlogopite or carbonate. Because the pressure of magma generation determines which volatile-mineral assemblage buffers the vapor composition, different liquids are produced at different pressures. The reactions

phlogopite + enstatite + sanidine + vapor $\rightleftarrows$ forsterite + liquid,

phlogopite + enstatite + sanidine + forsterite + vapor $\rightleftarrows$ liquid,

phlogopite + sanidine + forsterite + vapor $\rightleftarrows$ enstatite + liquid, and

phlogopite + kalsilite + enstatite + vapor $\rightleftarrows$ forsterite + liquid

characterize the beginning of melting of a phlogopite-bearing peridotite containing CO_2 and an amount of H_2O insufficient to hydrate all the potential phlogopite as a function of increasing pressure to 30 kb. The liquids produced vary in composition from quartz-normative at low pressures through enstatite-normative and leucite-normative to kalsilite-normative at high pressures. Liquid compositions change from tholeiitic to alkali basaltic at about 14 kb. This polybaric trend mimics the trend of liquids in the system $KAlSiO_4$–MgO–SiO_2–CO_2 (pt. 1, p. 385-420). The range of liquid compositions primarily results from an increase in the stability volume of enstatite at high pressure.

At pressures above 30 kb, a peridotite melts by either of the reactions

phlogopite + enstatite + magnesite + vapor $\rightleftarrows$ forsterite + liquid, or

phlogopite + enstatite + magnesite $\rightleftarrows$ forsterite + kalsilite + liquid

depending whether or not H_2O is present in sufficient amount to hydrate all the potential phlogopite. Pyrope appears as a reaction product at pressures in excess of approx 40 kb. Liquids produced are carbonatitic at pressures slightly above 30 kb but become increasingly potassic and silicic with increasing pressure as the hypersolidus stability range of phlogopite decreases.

At pressures in excess of 50 kb, phlogopite ceases to be a solidus phase. This pressure corresponds to the breakdown of phlogopite at subsolidus conditions and to the approximate intersection of the continental and Lesotho geotherms with the phlogopite + enstatite + magnesite solidus. Partial melting at higher pressures defined by the geotherm will not involve phlogopite.

The beginning of melting of a phlogopite-bearing spinel lherzolite for vapor-absent conditions has been determined to be 1075°C at 10 kb, 1125°C at 20 kb, and 1165°C at 30 kb. For H_2O-saturated conditions, the maximum stability of phlogopite in a spinel lherzolite composition containing 10 percent phlogopite is 1075°C at 10 kb, 1125°C at 20 kb, and 1150°C at 30 kb.

INTRODUCTION

Phlogopite is a common, if not essential, mineral in basic, potassium-rich magmas, kimberlites, and carbonatites. It is, moreover, present in

* Lunar and Planetary Institute, 3303 NASA Rd 1, Houston, Texas 77058

ultramafic nodules (Dawson and Powell, 1969; Jackson and Wright, 1970) and has been postulated as a source of mantle H_2O and K_2O (Kushiro, Syono, and Akimoto, 1967). Although it is known to have a wide range of stability (Yoder and Eugster, 1954; Markov and others, 1966; Kushiro, Syono, and Akimoto, 1967; Yoder and Kushiro, 1969; Yoder, 1970; Modreski and Boettcher, 1972, 1973), its possible role in the genesis of alkalic magmas is poorly understood, especially in the presence of a CO_2–H_2O vapor, which is now thought to be essential to alkalic magma genesis (Bailey, 1970; Yoder, 1970; Eggler, 1974, 1975a, 1976, 1978b; Eggler and Holloway, 1977; Wyllie and Huang, 1975a,b; Wyllie, 1977a,b).

To understand better the role of phlogopite in the genesis of alkalic magmas, melting relations of phlogopite at high pressures and temperatures have been investigated for natural and synthetic compositions. Experimental studies include determination of phlogopite stability in natural lherzolite compositions and on two joins in the system $KAlSiO_4$–MgO–SiO_2–H_2O–CO_2: the join $KMg_3AlSi_3O_{11}$–H_2O–CO_2 as a function of CO_2–H_2O vapor compositions, and the join $KMg_3AlSi_3O_{10}(OH)_2$–$MgSiO_3$–$MgCO_3$. A theoretical analysis of phlogopite stability for other bulk compositions in the system $KAlSiO_4$–MgO–SiO_2–H_2O–CO_2, in addition to the experimental results, enables the formulation of a comprehensive model for the role of phlogopite in the genesis of potassium-rich magmas. The synthetic system models a potassic peridotite containing phlogopite, magnesite, forsterite, enstatite, and pyrope, as well as the minor phases sanidine, kalsilite, and leucite. The last three phases are not subordinate in the role they may play in determining melt compositions where small degrees of partial melting are involved, as shown in part 1 of this paper.

EXPERIMENTAL METHODS

Starting Materials

Starting materials were natural and synthetic crystalline phases. Phlogopite and enstatite were crystallized from gels, prepared by the method of Luth and Ingamells (1965). Both phases were crystallized hydrothermally in cold seal pressure vessels, orthorhombic enstatite at 1.7 kb and 800°C for 3 weeks, and phlogopite at 1.4 kb and 800°C for 1 week. The phlogopite formed very fine grained crystalline aggregates less than 0.01 mm in average grain size. Powder X-ray diffraction patterns of the phlogopite and enstatite starting materials revealed no additional phases. Anhydrous phlogopite ("Ph"), $KMg_3AlSi_3O_{11}$, was prepared by firing phlogopite at 1100°C; powder X-ray diffraction indicated a phase assemblage of forsterite + kalsilite + leucite. Magnesite was a natural specimen provided by H. S. Yoder, Jr. The natural spinel lherzolite, provided by R. W. White to A. L. Boettcher, occurred as a nodule in nephelinite tuff, Salt Lake Crater, Oahu.

The K_2O and Na_2O contents of the phlogopite, analyzed by gravimetric and flame photometric procedures, respectively, are K_2O = 10.08 wt percent, and Na_2O = 0.18 wt percent (J. B. Bodkin analyst, Mineral

Constitution Labs, The Pennsylvania State Univ.). The slight Na_2O content is an impurity in the ludox sol used in gel preparation; K_2O in the original mixture was corrected for the sodium. The total alkali content of the phlogopite starting material is less than that of ideal phlogopite (11.29 wt percent). The loss is attributed to alkali volatilization during firing of the gel (1100°C for 13 hrs) and to alkali leaching by the vapor phase during hydrothermal crystallization.

The crystalline phases were ground by hand in acetone to −200 mesh. Starting compositions were prepared by mixing the crystalline phases either mechanically or by hand in acetone. The mixtures were then dried at 110°C, stored in corked vials, and redried prior to use.

Experimental Procedure

All runs were conducted in solid-media, high-pressure apparatus. Experiments on phlogopite-bearing spinel lherzolite compositions were conducted primarily at The Pennsylvania State University using 1.27 cm and 2.54 cm diam furnace assemblies and piston-in techniques (Boettcher and Wyllie, 1968). A −12 percent friction coefficient was applied for runs in the smaller diameter assemblies while a −6 percent correction was used for the 2.54 cm assemblies. Run procedures were similar to those detailed by Modreski and Boettcher (1972). All other experiments were conducted at the Geophysical Laboratory in 1.27 cm talc–pyrex and talc–boron nitride furnace assemblies (Boyd and England, 1960). Runs on spinel lherzolite compositions employed friction corrections. For other compositions at pressures less than or equal to 40 kb, a floating piston technique was used with no pressure correction for friction (for details, see pt. 1 of this paper). At 50 kb, the piston was run-in while warm to minimize brittle failure of the piston during the run-up procedure. In a typical run at 50 kb, pressure was applied to approx 35 kb, temperature was taken to approx 600°C, after 5 minutes pressure was advanced to the nominal pressure, and temperature was immediately taken to the nominal run temperature. For runs at 50 kb, piston support techniques were also required. In order to minimize the length of unsupported piston, a hardened steel support cylinder was shrunk fit on the base of a 1.27 cm diam carbide piston (Carboloy 999) and steel support rings (slip-fit tightness) were spaced above this. The length of the unsupported piston did not exceed 2 mm. Nominal pressures were maintained to ±0.1 kb for all experiments and are believed to be precise to ±0.5 kb.

Temperatures were measured with Pt_{100}–Pt_{90}–Rh_{10} thermocouples and automatically controlled to ±3°C at The Pennsylvania State University and to ±1°C at the Geophysical Laboratory (Hadidiacos, 1972). No corrections were made for the effect of pressure on the emf of the thermocouple.

Approximately 4 to 10 mg of the desired starting composition were welded in 2 mm diam $Pt_{95}Au_5$, 2.2 mm Pt, or $Ag_{50}Pd_{50}$ capsules with the desired proportion of volatiles. The $Ag_{50}Pd_{50}$ capsules were used at temperatures less than 1200°C for the Fe-bearing spinel lherzolite composi-

tions to reduce iron loss to the capsule. Carbon dioxide was added as silver oxalate, $Ag_2C_2O_4$ (Boettcher, Mysen, and Allen, 1973), while H_2O, other than structural water in phlogopite, was pipetted into the capsules with a microsyringe. Capsules containing volatiles were weighed prior to and after welding to ensure that volatiles were not lost. In order to minimize leaching of alkalies by H_2O-rich volatile compositions and formation of vapor quench phases, low volatile contents were employed where feasible; for example, only 10 wt percent H_2O was employed for the determination of phlogopite stability in spinel lherzolite for water-saturated conditions. This approach is justified for investigations at or near the solidus in the presence of a binary (H_2O–CO_2) vapor phase as well; however, it leads to some uncertainties in the vapor composition at conditions substantially above the solidus. Consequently, for investigations of the stability of phlogopite in the presence of a binary vapor phase, 25 wt percent total volatiles were used.

Run times varied from 1 to 78 hrs, depending on composition, physical conditions, and the presence and amount of volatiles. It was found that carbonate and phlogopite react rapidly, especially in the presence of volatiles, while the natural spinel lherzolite reacts much slower.

Phase Identification

Phase identification was accomplished principally by petrographic microscope and powder X-ray diffraction. Descriptions and criteria for the identification of phases occurring in runs involving the spinel lherzolite have been discussed by Mysen and Boettcher (1975a) and in runs where phlogopite is present by Modreski and Boettcher (1972) and Yoder and Kushiro (1969). The criteria of Yoder and Kushiro for distinguishing the stable and quench habits of phlogopite were particularly helpful where quenching problems are serious in the water-rich portions of the system $KMg_3AlSi_3O_{11}$–H_2O–CO_2. Only the 1M or 3T polymorph of phlogopite and the orthorhombic polymorph of enstatite were observed.

The identification of kalsilite, sanidine, and leucite was, almost without exception, accomplished by powder X-ray diffraction techniques. The textural habits of these phases are sufficiently obscure as to make optical confirmation difficult; although they may poikilitically enclose abundant forsterite grains, they also occur as small inclusions in other phases and in glass of similar low refractive index.

The extent of development of quench phlogopite precluded meaningful reversal runs in the H_2O-rich portions of the system. The amount of quench crystals decreased dramatically with increasing CO_2 contents to approx $X_{CO_2} = 0.5$, at which point liquid quenched to glass. The solidus at 20 kb for the H_2O-deficient melting of phlogopite and the upper boundaries of the phlogopite melting intervals for the spinel lherzolite compositions were reversed.

Quench carbonates were encountered in runs in the composition join phlogopite–enstatite–magnesite. The criteria for discriminating stable carbonate grains from grains quenched from liquid have been well

TABLE 1

Result of experiments on spinel lherzolite + 10% phlogopite composition

Run no.	P (kb)	T (°C)	H_2O (wt %)	Duration (hr)	Assemblage
85-P*	10	1055	--	6	Ol,Opx,Cpx,Ph,Sp
82-P	10	1075	--	19.25	Ol,Opx,Cpx,Ph,Sp,L(tr)
80-P	10	1100	--	19.5	Ol,Opx,Cpx,Ph,Sp,L
77-P	10	1130	--	23	Ol,Opx,Cpx,Sp,L
66-P	10	1070	9.71	12	Ol,Opx,Cpx,Ph,Sp,Amph,V,L
64-P	10	1090	9.45	24	Ol,Opx,Cpx,Sp,Amph(tr),V,L
63-P	10	1110	10.04	22	Ol,Opx,Cpx,Sp,V,L
74-P	15	1060	--	23	Ol,Opx,Cpx,Ph,Sp
72-P	15	1080	--	21.5	Ol,Opx,Cpx,Ph,Sp
71-P	15	1100	--	23	Ol,Opx,Cpx,Ph,Sp
76-P	15	1125	--	21.5	Ol,Opx,Cpx,Ph,Sp,L
69-P	15	1150	--	22	Ol,Opx,Cpx,Ph(tr),Sp,L
70-P**	15	1150	--	18.25	Ol,Opx,Cpx,Ph(tr),Sp,L
73-P	15	1170	--	21	Ol,Opx,Cpx,Sp,L
75-P	15	1190	--	2	Ol,Opx,Cpx,Sp,L
88-P***	15	1170/1130	--	21/23	Ol,Opx,Cpx,Ph,Sp,L
28-P	15	950	9.95	78	Ol,Opx,Cpx,Ph,Sp,Amph,V,L
30-P	15	970	9.98	24	Ol,Opx,Cpx,Ph,Sp,Amph,V,L
32-P	15	990	9.91	25.5	Ol,Opx,Cpx,Ph,Sp,Amph,V,L
34b-P	15	1010	10.02	24.75	Ol,Opx,Cpx,Ph,Sp,Amph,V,L
29-P	15	1050	9.94	23	Ol,Opx,Cpx,Ph,Sp,Amph,V,L
31b-P	15	1070	10.17	20	Ol,Opx,Cpx,Ph,Sp,Amph,V,L
37-P	15	1090	9.85	24	Ol,Opx,Cpx,Ph,Sp,Amph,V,L
40-P	15	1110	9.91	21	Ol,Opx,Cpx,Ph(tr),Sp,V,L
67-P	15	1130	10.04	18	Ol,Opx,Cpx,Sp,V,L
87-P***	15	1130/1090	10.22	18/15	Ol,Opx,Cpx,Ph,Sp,Amph(tr),V,L
36b-P	18	980	9.85	38	Ol,Opx,Cpx,Ph,Sp,Amph,V,L
84a-P	20	1130	--	20	Ol,Opx,Cpx,Ph,Sp
81-P	20	1150	--	20.25	Ol,Opx,Cpx,Ph(tr),Sp,L
83-P	20	1170	--	2.25	Ol,Opx,Cpx,Ph,Sp,L
78-P	20	1190	--	2.25	Ol,Opx,Cpx,Ph(?),Sp,L
25b-P	20	1000	9.82	24.5	Ol,Opx,Cpx,Ph,Sp(tr),Gt(tr),Amph,V,L
26b-P	20	1070	10.00	24	Ol,Opx,Cpx,Ph(tr),Sp,Amph,V,L
38-P	20	1110	10.03	20	Ol,Opx,Cpx,Ph,Sp,Amph(tr),V,L
84b-P	20	1130	10.23	20	Ol,Opx,Cpx,Sp,V,L
79-P	20	1150	9.62	20.75	Ol,Opx,Cpx,Sp,V,L
33b-P	25	1050	10.00	24	Ol,Opx,Cpx,Ph,Gt,V,L
35b-P	25	1100	10.03	21	Ol,Opx,Cpx,Ph,Sp,Gt(tr),V,L
116	30	1150	--	19	Ol,Opx,Cpx,Ph,Gt
120	30	1175	--	19.5	Ol,Opx,Cpx,Ph,Gt,L
115	30	1200	--	14	Ol,Opx,Cpx,Ph,Gt,L
121	30	1230	--	22	Ol,Opx,Cpx,Ph,Gt,L
119	30	1260	--	18.5	Ol,Opx,Cpx,Gt,L
124	30	1125	9.59	14.5	Ol,Opx,Cpx,Ph,Gt,V,L
125	30	1150	9.39	10.25	Ol,Opx,Cpx,Gt,V,L

* P denotes runs done at The Pennsylvania State University.

** Same as run no. 69-P.

*** Reversal.

Abbreviations: Ol, olivine; Opx, orthopyroxene; Cpx, clinopyroxene; Ph, phlogopite; Sp, spinel; Gt, garnet; Amph, amphibole; L, liquid; V, vapor; (tr), trace amounts; (?), possibly present.

TABLE 2
Results of experiments on

Run no.	Reactants (wt %)	P (kb)	T (°C)	H_2O^* (wt %)	CO_2 (wt %)	$X_{CO_2}^*$	Duration (hr)	Assemblage
				A. Ph-H_2O				
177	Ph	20	1175	20.10			2	Ph,Fo,V
174	Ph	20	1200	19.44			1.5	Ph,Fo,V
169	Ph	20	1200	14.06			2.5	Ph,Fo,V
171	Ph	20	1225	14.04			1.75	Ph,Fo,L
178	Ph	20	1225	20.00			2	Fo,L,V
184	Ph	20	1225	20.92			2.5	Fo,L,V
185	Ph	20	1225	21.80			2.75	Fo,L,V
194	Ph	20	1225	16.67			2	Fo,L,V
192	Ph	20	1250	17.86			1.75	Fo,L,V
191	Ph	20	1250	15.40			1.75	Ph(tr),Fo,L
182	Ph	20	1250	20.00			3	Fo,L,V
176	Ph	20	1250	14.15			2	Ph,Fo,L
180	Ph	20	1275	15.98			3.17	Fo,L
187	Ph	20	1275	20.13			2	Fo,L,V
193	Ph	20	1275	14.14			1.75	Ph,Fo,L
181	Ph	20	1300	15.88			2.5	Fo,L
190	Ph	20	1300	13.20			1	Fo,L
186	Ph	20	1325	14.08			2	Fo,L
189	Ph	20	1325	7.51			2	Ph(tr),Fo,L
204	Ph	20	1325	--			2	Ph,Fo,L(tr)
170	Ph	20	1350	--			2	Fo,L
173	Ph	20	1370	--			1.75	Fo,L
				B. $(Ph)_{75}$-$(X_{CO_2})_{25}$				
151	Ph	20	1175	--	24.39	1	2	Ph,Fo(tr),L(?),V
149	Ph	20	1200	--	25.26	1	2.25	Ph,Fo,L,V
208	Ph	20	1200	11.90	13.03	.310	2	Ph,Fo,V
230	Ph	20	1200	1.19	25.81	.899	2.5	Ph,Fo,L(tr),V
195	Ph	20	1225	9.17	22.02	.496	2	Ph,Fo,V
206	Ph	20	1225	12.08	12.55	.298	1.25	Ph,Fo,L,V
229	Ph	20	1225	2.37	23.26	.801	3	Ph,Fo,L,V
203	Ph	20	1225	--	25.66	1	2.5	Ph,Fo,L,V
175	Ph	20	1250	6.92	16.91	.500	2.5	Ph,Fo,L,V
205	Ph	20	1250	5.26	19.88	.607	2	Ph,Fo,V
216	Ph	20	1250	12.30	12.57	.295	2.25	Ph,Fo,L,V
218	Ph	20	1250	2.35	24.06	.807	2	Ph,Fo,L,V
219	Ph	20	1250	3.70	21.55	.704	2	Ph,Fo,V
222	Ph	20	1275	12.51	12.86	.296	2	Fo,L,V
209	Ph	20	1275	5.72	20.95	.600	2	Ph,Fo,V
210	Ph	20	1275	3.82	21.46	.697	2	Ph,Fo,L(tr),V
179	Ph	20	1275	6.98	16.96	.498	3	Ph,Fo,L,V
183	Ph	20	1300	6.94	17.01	.501	2	Ph,Fo,L,V(?)
212	Ph	20	1300	5.16	19.17	.603	1.5	Ph,Fo,L,V
213	Ph	20	1300	4.19	21.98	.682	1.75	Ph,Fo,L,V
220	Ph	20	1300	4.53	20.13	.645	1.75	Ph,Fo,V

Ph–H_2O, $(Ph)_{75}$–$(X_{CO_2})_{25}$, and ("Ph"–Ph)$_{93}$–$(CO_2)_7$

Run no.	Reactants (wt %)	P (kb)	T (°C)	H_2O (wt %)	CO_2 (wt %)	X_{CO_2}	Duration (hr)	Assemblage
227	Ph	20	1300	2.21	23.22	.811	1.75	Ph,Fo,L,V
228	Ph	20	1300	2.96	22.62	.757	2	Ph,Fo,L,V
154	Ph	20	1300	--	24.83	1	1.5	Ph,Fo,L,V
160	Ph	20	1325	--	24.80	1	1.25	Fo,L,V
207	Ph	20	1325	5.16	19.90	.612	1.5	Ph(tr),Fo,L,V
196	Ph	20	1325	6.40	16.98	.502	2	Fo,L,V
			C.	("Ph"-Ph)$_{93}$-$(CO_2)_7$				
265	"Ph"$_{40.31}$-Ph$_{59.61}$	20	1150		7.02	1	3	Ph,Fo,Ks,Lc,V
260	"Ph"$_{95.21}$-Ph$_{4.79}$	20	1150		6.93	1	2.5	Ph(tr),Fo,Ks,Lc,V
252	"Ph"$_{66.60}$-Ph$_{33.40}$	20	1150		7.13	1	2.5	Ph,Fo,Ks,Lc,V
250	"Ph"$_{90.29}$-Ph$_{9.71}$	20	1175		7.06	1	3.5	Fo,Ks,Lc,L,V
253	"Ph"$_{59.84}$-Ph$_{40.16}$	20	1175		7.06	1	3	Fo,Ks(tr),Lc,L,V
255	"Ph"$_{70.97}$-Ph$_{29.03}$	20	1175		6.96	1	3	Fo,Ks,Lc,L,V
405**	"Ph"$_{75}$-Ph$_{25}$	20	1175/1150		6.84	1	2/2	Ph,Fo,Ks,Lc,V
257***	"Ph"	20	1200		6.85	1	4	Fo,Ks,Lc,V
259	"Ph"	20	1200		7.92	1	2	Fo,Ks,Lc,V
231	"Ph"$_{35.27}$-Ph$_{64.73}$	20	1200		6.98	1	2.75	Ph,Fo,L(tr),V
233	"Ph"$_{16.43}$-Ph$_{83.57}$	20	1225		6.93	1	3.25	Ph,Fo,L,V
237	"Ph"$_{50}$-Ph$_{50}$	20	1225		7.02	1	2	Ph,Fo,L,V
246	"Ph"$_{69.79}$-Ph$_{30.21}$	20	1225		7.02	1	2.25	Fo,Ks,Lc,L,V
248	"Ph"	20	1225		7.01	1	2.5	Fo,Ks,Lc,V
249	"Ph"$_{63.08}$-Ph$_{36.92}$	20	1225		6.66	1	2	Fo,Ks,Lc(?),L,V
262	"Ph"$_{79.72}$-Ph$_{20.28}$	20	1250		6.90	1	2.25	Fo,Ks,Lc(?),L,V
263****	"Ph"	20	1275		6.82	1	2	Fo,Ks,Lc,L(?),V
239	"Ph"	20	1275		6.75	1	2	Fo,Ks,Lc,V
234	"Ph"$_{20}$-Ph$_{80}$	20	1275		7.11	1	2.25	Ph,Fo,L,V
258	"Ph"$_{60.16}$-Ph$_{39.84}$	20	1275		7.01	1	1	Fo,Ks,Lc(?),L,V
238	"Ph"$_{25.19}$-Ph$_{74.81}$	20	1300		7.18	1	1.5	Ph,Fo,L,V
240	"Ph"$_{37.40}$-Ph$_{62.60}$	20	1300		7.01	1	2	Ph,Fo,L,V
242	"Ph"$_{50}$-Ph$_{50}$	20	1300		7.01	1	1.5	Fo,L,V
261	"Ph"	20	1300		6.82	1	2	Fo,Ks,L,V
156	"Ph"	20	1325		10.31	1	2	Fo,Ks,L,V
268	"Ph"$_{74.44}$-Ph$_{25.56}$	20	1325		7.06	1	2	Fo,Ks(tr),L,V
270	"Ph"$_{77.59}$-Ph$_{22.51}$	20	1350		6.94	1	2.25	Fo,Ks,L,V
271	"Ph"	20	1350		6.97	1	2	Fo,Ks,L,V
266	"Ph"	20	1375		7.10	1	2	Fo,Ks(tr),L,V
272	"Ph"$_{71.43}$-Ph$_{28.57}$	20	1375		10.21	1	2	Fo,L,V
274	"Ph"	20	1400		7.11	1	2	Fo,L,V
275	"Ph"$_{61.28}$-Ph$_{38.72}$	30	1150		10.00	1	2.25	Ph,Fo,Ks,Mag,En,V

* Excludes structural H_2O.
** Reversal.
*** Same as run no. 259.
**** Same as run no. 239.

Abbreviations: Ph, phlogopite; "Ph", anhydrous phlogopite; Fo, forsterite; Ks, kalsilite; Lc, leucite; Sa, sanidine; En, enstatite; Mag, magnesite; Pyr, pyrope; L, liquid; V, vapor; (tr), trace amounts; (?), possibly present.

characterized previously (Wyllie and Tuttle, 1960; Boettcher and Wyllie, 1968).

EXPERIMENTAL RESULTS

In tables 1, 2, and 3, the details of experimental runs are summarized as a function of increasing pressure within subgroups corresponding to the three principal areas of investigation.

Spinel Lherzolite + 10 percent Phlogopite

The spinel lherzolite selected for this aspect of the investigation (618-138b.1) was described by White (1966), and the high pressure phase relations and phase geochemistries were determined by Mysen and

TABLE 3
Results of experiments on Ph–En–Mag

Run no.	Reactants (wt %)	P (kb)	T (°C)	Duration (hr)	Assemblage
384	$Ph_{33}En_{33}Mag_{33}$	25	1000	2	Ph(tr),Fo,Ks,Mag,V
429	$Ph_{16}En_{16.5}Mag_{67.5}$	25	1050	2	Fo,Mag,Ks(?),V
386	$Ph_{33}En_{33}Mag_{33}$	26.25	1000	2.5	Ph,Fo(tr),Mag,En
383	$Ph_{33}En_{33}Mag_{33}$	27.5	1000	4	Ph,Fo(tr),Mag,En
389	$Ph_{33}En_{33}Mag_{33}$	27.5	1100	2.5	Fo,Ks,V
377	$Ph_{33}En_{33}Mag_{33}$	27.5	1150	2.5	Ph(tr),Fo,En,Ks(?),V
387	$Ph_{33}En_{33}Mag_{33}$	28.75	1100	2.5	Ph,Fo(tr),Mag,En
385	$Ph_{33}En_{33}Mag_{33}$	30	1100	2.25	Ph,Fo(tr),Mag,En
379	$Ph_{33}En_{33}Mag_{33}$	30	1150	2.25	Ph,Fo,Ks(tr),Mag,En,V
381	$Ph_{33}En_{33}Mag_{33}$	32.5	1150	2	Ph,Fo(tr),Mag,En
420	$Ph_{16}En_{16.5}Mag_{67.5}$	32.5	1165	2	Ph,Fo,L(?),Mag,En
388	$Ph_{33}En_{33}Mag_{33}$	32.5	1190	2.75	Ph,Fo(tr),L(tr),Mag,En
412	$Ph_{16.7}En_{15.6}Mag_{66.7}$	32.5	1215	1.25	Ph(tr),Fo,En,L
382	$Ph_{33}En_{33}Mag_{33}$	32.5	1225	2	Ph,Fo,L
413	$Ph_{16.7}En_{15.6}Mag_{66.7}$	32.5	1250	1.5	Fo,L
417	$Ph_{33.1}En_{32.7}Mag_{34.2}$	32.5	1275	1.5	Ph,Fo,En(?),L
415	$Ph_{16}En_{16.5}Mag_{67.5}$	32.5	1300	1.25	Fo,L
419	$Ph_{33.1}En_{32.7}Mag_{34.2}$	32.5	1325	1	Ph,Fo,En(?),L
418	$Ph_{16}En_{16.5}Mag_{67.5}$	40	1200	1.5	Ph,Fo(tr),Mag,En
416	$Ph_{16}En_{16.5}Mag_{67.5}$	40	1250	1.25	Mag,En,Pyr,Fo(tr),L(tr)
443	$Ph_{33.1}En_{32.7}Mag_{34.2}$	40	1250	2	Ph,Fo,En,Pyr(tr),L
427	$Ph_{16}En_{16.5}Mag_{67.5}$	50	1100	1.5	Ph,En,Mag,Fo(tr)
438	$Ph_{33}En_{33}Mag_{33}$	50	1200	1.5	Ph,Fo,Mag,En
440	$Ph_{16}En_{16.5}Mag_{67.5}$	50	1250	1.5	Fo,En,Mag,Pyr(?),L
439	$Ph_{33}En_{33}Mag_{33}$	50	1260	2	Fo(tr),Mag,En,Pyr,L
401*	$Ph_{33}En_{33}Mag_{33}$	27.5/30	1100	2/2	Ph,Mag,En,Fo(tr),Ks(tr),V

* Reversal.
Abbreviations as in table 2

Boettcher (1975a,b) as a function of controlled fugacities of H_2O, CO_2, and H_2. To this spinel lherzolite was added 10 wt percent synthetic, crystalline phlogopite. The composition of the spinel lherzolite and of the starting composition (and their respective CIPW norms) are presented in table 4. The principal effect of adding 10 percent phlogopite is to increase the K_2O content from 0.01 to 1.02 wt percent and the normative Or from 0.06 to 6.03 wt percent. The melting relations of the starting material for vapor-absent conditions are presented in figure 1. Based on experimental results in synthetic systems, Modreski and Boettcher (1972) observed that the stability of phlogopite at upper mantle condi-

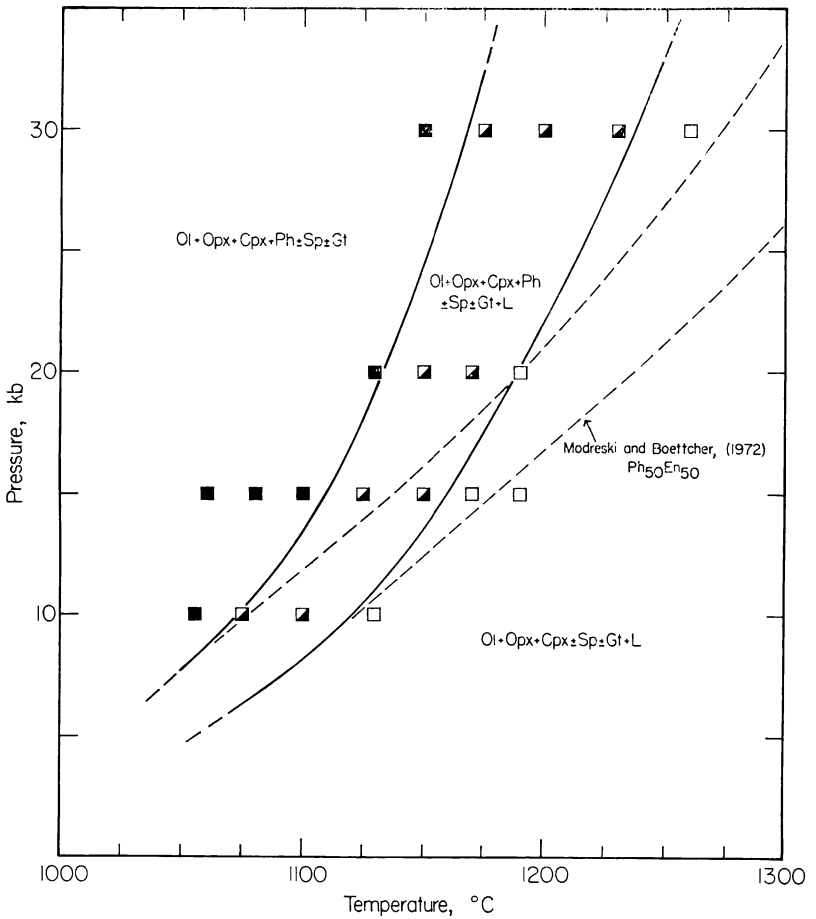

Fig. 1. Stability of phlogopite in the composition spinel lherzolite + 10 wt percent phlogopite for volatile-absent conditions. The stability of phlogopite as determined by Modreski and Boettcher (1972) for the composition $Ph_{50}En_{50}$ (wt percent) is summarized for comparative purposes. Abbreviations: Ol, olivine; Cpx, clinopyroxene; Opx, orthopyroxene; Ph, phlogopite; Amph, amphibole; Gt, garnet; Sp, spinel; L, liquid; V, vapor; solid squares, subsolidus region; partially solid squares, phlogopite melting interval; open squares, phlogopite-absent melting region.

TABLE 4
Lherzolite starting composition

	Spinel lherzolite*	Synthetic phlogopite**	Lherzolite + 10% phlogopite
SiO_2	43.7	43.7	43.7
TiO_2	0.20	--	0.18
Al_2O_3	4.00	12.4	4.84
Fe_2O_3	0.89	--	0.80
FeO	8.09	--	7.28
MgO	37.4	29.3	36.6
CaO	3.50	--	3.15
Na_2O	0.38	0.18	0.36
K_2O	0.01	10.08	1.02
H_2O^+	0.14	4.32	0.56
H_2O^-	0.10	--	0.09
P_2O_5	(tr)	--	(tr)
MnO	0.123	--	0.111
Cr_2O_3	0.40	--	0.36
NiO	0.24	--	0.22
Totals	99.17	100	99.26
		CIPW norm	
Or	0.06		6.03
Ab	3.22		3.05
An	9.18		8.58
Di	6.41		5.51
(Di)	(5.77)		(5.01)
Hy	13.36		5.73
(Fs)	(1.34)		(0.52)
(En)	(12.02)		(5.21)
Ol	64.20		67.45
(Fa)	(6.42)		(6.07)
(Fo)	(57.78)		(61.38)
Mag	1.29		1.16
Ilm	0.38		0.34
Ap	(tr)		(tr)
Cr	0.59		0.53
TT index	3.27		9.07
FeO/(FeO+MgO)†	0.10		0.09

* 618-138b.1 peridotite (spinel lherzolite), Hawaii (White, 1966). Analyst: N. H. Suhr, The Pennsylvania State University.

** Phlogopite analysis recalculated to correct for alkali loss during synthesis. K_2O and Na_2O determined by J. B. Bodkin, The Pennsylvania State University.

† Molar ratio.

tions is modeled most closely by the assemblage phlogopite + enstatite, and their results for the composition phlogopite$_{50}$–enstatite$_{50}$ (wt percent) are also reproduced in figure 1 for comparison. With increasing pressure, the departure between the two sets of curves increases. At pressures of about 30 kb, the net effect of the additional components in the natural system, relative to the results of Modreski and Boettcher in the system K_2O–MgO–Al_2O_3–SiO_2–H_2O, is to reduce the stability of phlogopite by approx 100°C.

The solidus for the phlogopite–spinel lherzolite represents the beginning of melting in the upper mantle for vapor-absent conditions. The solidus was determined principally by the presence of glass. This criterion is not unambiguous as phlogopite may decompose at temperatures below the solidus, in response to the presence of pore space in the charge, producing traces of melt. It was observed that the abundance of phlogopite decreases markedly at the solidus and that hypersolidus phlogopite was characteristically subhedral to anhedral (euhedral at temperatures below the solidus); consequently, the abundances and textural appearances of phlogopite were also employed as criteria for determining the beginning of melting.

Spinel Lherzolite + 10 percent Phlogopite + H_2O

The stability of phlogopite in natural spinel lherzolite in the presence of excess H_2O-rich vapor is presented in P–T projection in figure 2. Modreski and Boettcher's (1972) results for phlogopite$_{50}$–enstatite$_{50}$ + H_2O are also summarized. As was observed in the absence of a vapor phase, the departure between the two sets of results increases with increasing pressure. This difference is in accord with the estimation of Modreski and Boettcher (1972) regarding the effect of additional components such as Ti and Fe on phlogopite stability.

Average electron microprobe analyses of phlogopites are presented in table 5. These are compared with average compositions of primary phlogopites from lherzolite nodules in kimberlites. The run phlogopites are highly aluminous and show substantial solution toward eastonite, $KMg_{2.5}Al_2Si_{2.5}O_{10}(OH)_2$. The analyses also show a slight deficiency in potassium and magnesium. Compositional variations as a function of pressure are slight; with increasing pressure, TiO_2 decreases marginally, while Cr_2O_3 and FeOt (total iron as FeO) increase. Edgar, Green, and Hibberson (1976) also reported that the TiO_2 content of phlogopite crystallized in a biotite mafurite decreases with increasing pressure. The principal compositional differences between the phlogopite analyses obtained from experimental runs and those of Carswell (1975) and Dawson and Smith (1975) from kimberlites are the higher Al_2O_3 and lower MgO and FeOt in the former. The low TiO_2 and FeOt and high Cr_2O_3 contents are typical of mantle lherzolite-derived micas and are distinct from Ti- and Fe-enriched and Cr-poor megacrysts and secondary phlogopites from kimberlites (Dawson and Smith, 1975).

The appearance of garnet and disappearance of amphibole are also indicated in figure 2. These phase relations are not significantly different from the results of Mysen and Boettcher (1975a). Amphibole is inferred to be a tschermakitic to pargasitic hornblende and is stable to approx 22 kb and 1100°C. The thermal stability of amphibole exceeds that of phlogopite at pressures less than 12 kb. Mysen and Boettcher (1975b) report that as much as 1 wt percent K_2O may be contained in amphibole coexisting with phlogopite; amphibole compositions were not investigated in this study.

The Composition Join $KMg_3AlSi_3O_{11}$–H_2O–CO_2

The join $KMg_3AlSi_3O_{11}$–H_2O–CO_2 was investigated at 20 kb to determine the stability of phlogopite as a function of H_2O–CO_2 volatile

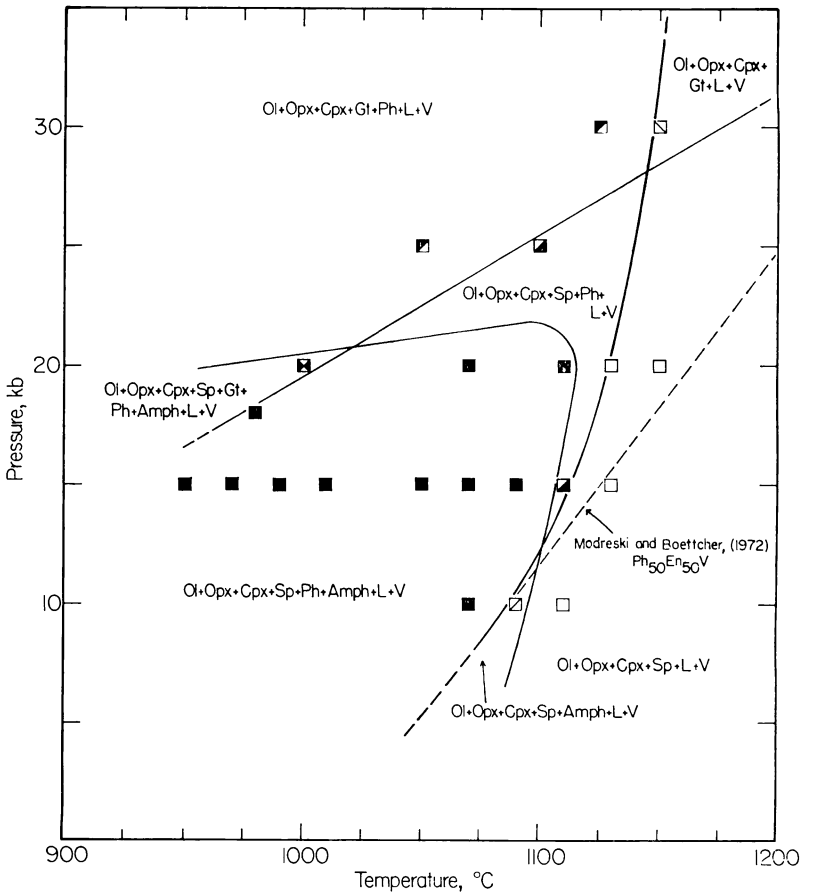

Fig. 2. Stability of phlogopite in the composition spinel lherzolite + 10 wt percent phlogopite for water-saturated conditions. The stability of phlogopite as determined by Modreski and Boettcher (1972) for the composition $Ph_{50}En_{50}V$ (wt percent; V denotes excess water conditions) is summarized for comparative purposes. Phase abbreviations are the same as figure 1. Closed and partially closed run symbols are within the phlogopite stability field. Open run symbols are in phlogopite-absent melting regions.

composition. Compositions on the join can be considered conveniently in terms of five components, $KAlSiO_4$–Mg_2SiO_4–SiO_2–H_2O–CO_2; slight solution of excess alumina in phlogopite has been observed at higher pressures by Modreski and Boettcher (1973).

Two compositional regions exist in the join $KMg_3AlSi_3O_{11}$–H_2O–CO_2, a region of high a_{H_2O} and a region of low a_{H_2O}, which are characterized by different liquids and different melting reactions. Three 20 kb sections have been investigated in detail to define and contrast these two melting regions (fig. 3). The sections investigated include a CO_2-absent join $KMg_3AlSi_3O_{11}$–H_2O (fig. 4), detailed previously by Yoder

TABLE 5
Phlogopite compositions

Run no.:	32-P	25b-P	33b-P	Primary phlogopites from lherzolite nodules in kimberlites	
H_2O (wt %):	9.91	9.82	10.00		
P (kb):	15	20	25		
T (°C):	990	1000	1050		
No. of analyses	3	6	2	5*	2**
SiO_2	40.9	40.5	41.0	41.3	42.0
TiO_2	0.68	0.63	0.54	0.32	0.53
Al_2O_3	15.5	17.0	16.0	12.6	11.6
FeO†	1.89	1.92	2.38	2.63	2.56
MgO	25.1	24.8	24.7	26.8	26.1
MnO	0.06	0.08	0.10	0.02	0.01
Na_2O	0.33	0.54	0.31	0.74	0.18
K_2O	9.64	9.20	9.84	9.36	10.6
NiO	0.25	0.12	0.15	n.d.	0.25
Cr_2O_3	0.69	0.73	0.82	0.70	0.68
Totals	95.0	95.6	95.8	94.5	94.5
		Chemical formulae (O = 22)			
Si	5.740	5.637	5.723		
Ti	0.072	0.067	0.057		
Al	2.561	2.789	2.625		
Fe††	0.221	0.227	0.279		
Mg	5.255	5.147	5.146		
Mn	0.007	0.009	0.012		
Na	0.091	0.144	0.084		
K	1.726	1.635	1.750		
Ni	0.028	0.014	0.017		
Cr	0.076	0.081	0.089		
Totals	15.777	15.750	15.782		

* Average of five primary phlogopites (Carswell, 1975).

** Average of two primary phlogopites; one from xenolith 1141 from Bulfontein and the other from DeBeers (Dawson and Smith, 1975).

† Total Fe determined as FeO.

†† Formula calculation based on Fe^{2+}.

and Kushiro (1969) at 10 kb; the join $KMg_3AlSi_3O_{10}(OH)_2$ + 25 percent H_2O–$KMg_3AlSi_3O_{10}(OH)_2$ + 25 percent CO_2 (fig. 5), which illustrates the stability of phlogopite as a function of X_{CO_2} when there are large quantities of volatiles present; and the join $KMg_3AlSi_3O_{10}(OH)_2$ + 7 percent CO_2–$KMg_3AlSi_3O_{11}$ + 7 percent CO_2 (fig. 6), which depicts phlogopite stability in the presence of a multicomponent vapor with insufficient H_2O to hydrate all the potential phlogopite. From these data, two additional sections have been compiled; figure 7A is an isobaric section at 20 kb across both compositional regions, and figure 7B is an isobaric-isothermal section at 20 kb and 1250°C.

$KMg_3AlSi_3O_{11}$–H_2O.—Details on this join (fig. 4) are similar to the join at 10 kb by Yoder and Kushiro (1969). Two compositional regions exist that are characterized by distinctly different liquids. The first region contains sufficient H_2O to saturate the phlogopite in the system, whereas the second region contains insufficient H_2O to hydrate the phlogopite. The latter region is characterized by the coexistence of phlogopite with its breakdown products, kalsilite, forsterite, and leucite, at subsolidus temperatures. This assemblage melts in univariant fashion to a liquid whose composition is independent of the H_2O content of the

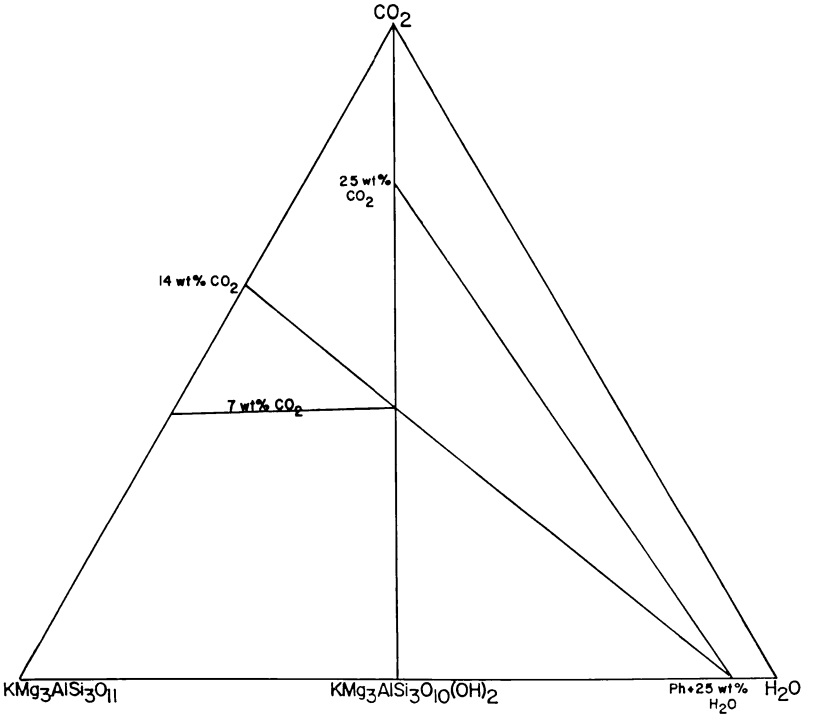

Fig. 3. The composition triangle, $KMg_3AlSi_3O_{11}$–H_2O–CO_2. The location of sections investigated at 20 kb and presented in figures 4, 5, and 6 and the orientation of the compilation isobar (fig. 7A) are shown. Figure 3 is presented in mol percent; however, the end points of the various joins are located by their wt percent equivalent.

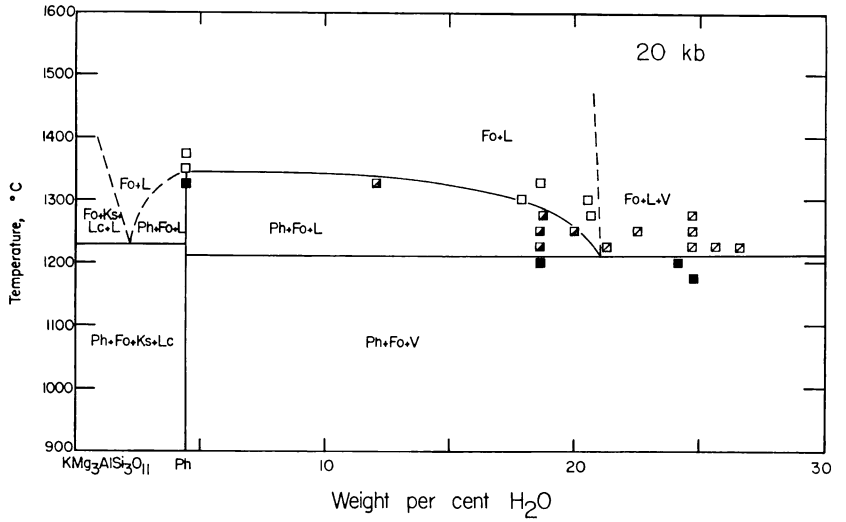

Fig. 4. Results of quenching experiments at 20 kb on the join $KMg_3AlSi_3O_{11}$–H_2O. The solidus for compositions containing less H_2O than phlogopite is from Yoder and Kushiro (1969). Dashed boundaries are inferred. Abbreviations: Fo, forsterite; Ph, phlogopite; Ks, kalsilite; Lc, leucite; L, liquid; V, vapor.

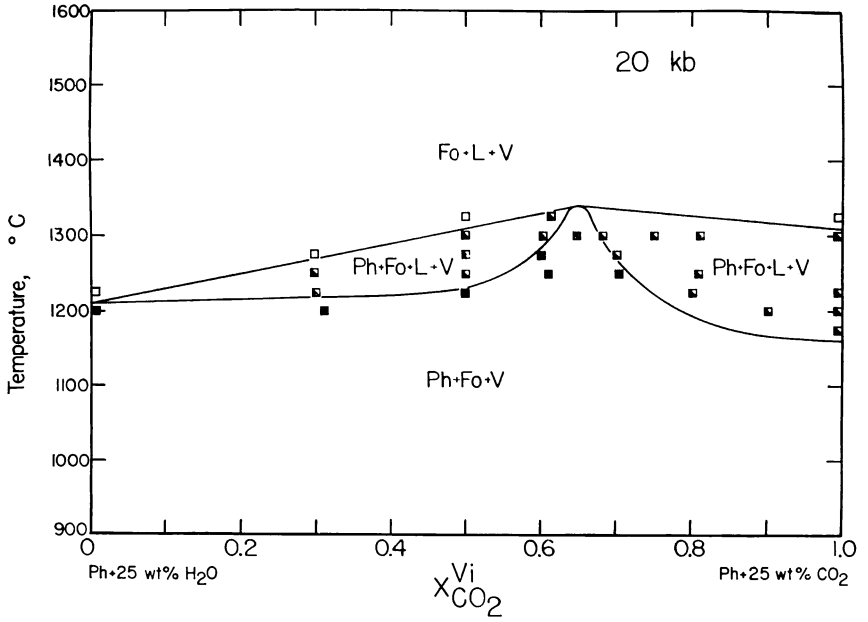

Fig. 5. Results of quenching experiments at 20 kb on the section $KMg_3AlSi_3O_{10}(OH)_2$ + 25 percent H_2O–$KMg_3AlSi_3O_{10}(OH)_2$ + 25 percent CO_2. The abscissa denotes the composition of volatiles, excluding structural H_2O, added to the phlogopite. The location of the section is given in figure 3. Abbreviations are the same as figure 4.

join as long as buffering conditions are maintained. Phase relations in this portion of figure 4, not determined because of the large uncertainty involved in adding small quantities of H_2O to the experimental charges, have been extrapolated from the results of Yoder and Kushiro (1969) at 10 kb. Their melting reaction,

$$\text{phlogopite} + \text{kalsilite} + \text{leucite} \rightleftarrows \text{forsterite} + \text{liquid}, \quad (1)$$

occurs at approx 1230°C at 20 kb. Melting behavior in this compositional region persists in a slightly modified fashion when CO_2 is added to the system, and it will be argued below that the resulting reaction is potentially important to phlogopite stability in the upper mantle and to the role of phlogopite in magma genesis.

In the absence of a vapor phase at 20 kb, but with just sufficient H_2O to saturate all the phlogopite, phlogopite melts by the reaction

$$\text{phlogopite} \rightleftarrows \text{forsterite} + \text{liquid} \quad (2)$$

at 1340° ± 12°C. In the presence of a water-rich vapor, phlogopite melts at 1210° ± 12°C; the reaction is univariant because of the compositional restriction of kalsilite indifference (the liquid is coplanar with forsterite, phlogopite, and vapor). The results on the join phlogopite–H_2O compare favorably with the previous determinations of Yoder and Kushiro (1969).

$KMg_3AlSi_3O_{10}(OH)_2$ + 25 percent H_2O–$KMg_3AlSi_3O_{10}(OH)_2$ + 25 percent CO_2.—Yoder (1970) investigated two isobaric, isothermal sections

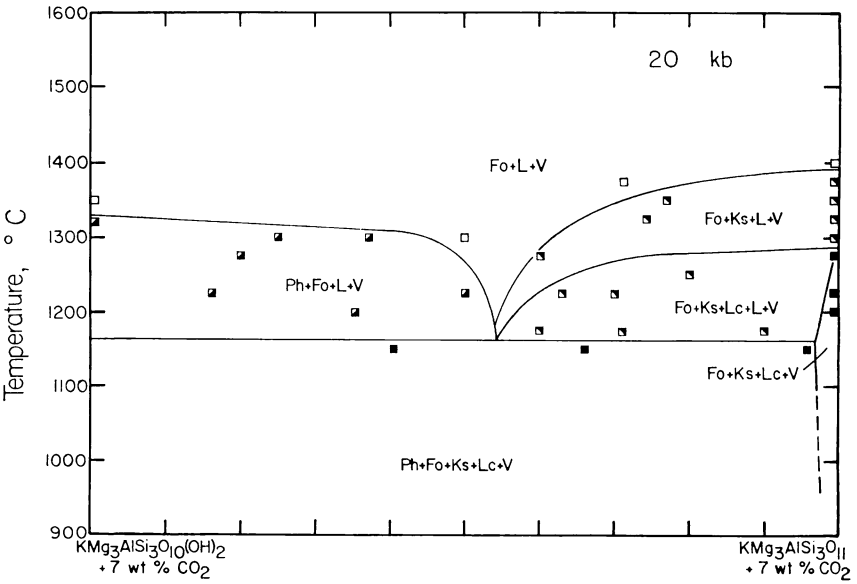

Fig. 6. Results of quenching experiments at 20 kb on the section $KMg_3AlSi_3O_{10}(OH)_2$ + 7 percent CO_2–$KMg_3AlSi_3O_{11}$ + 7 percent CO_2 (wt percent). The location of the join is given in figure 3. Abbreviations are the same as figure 4.

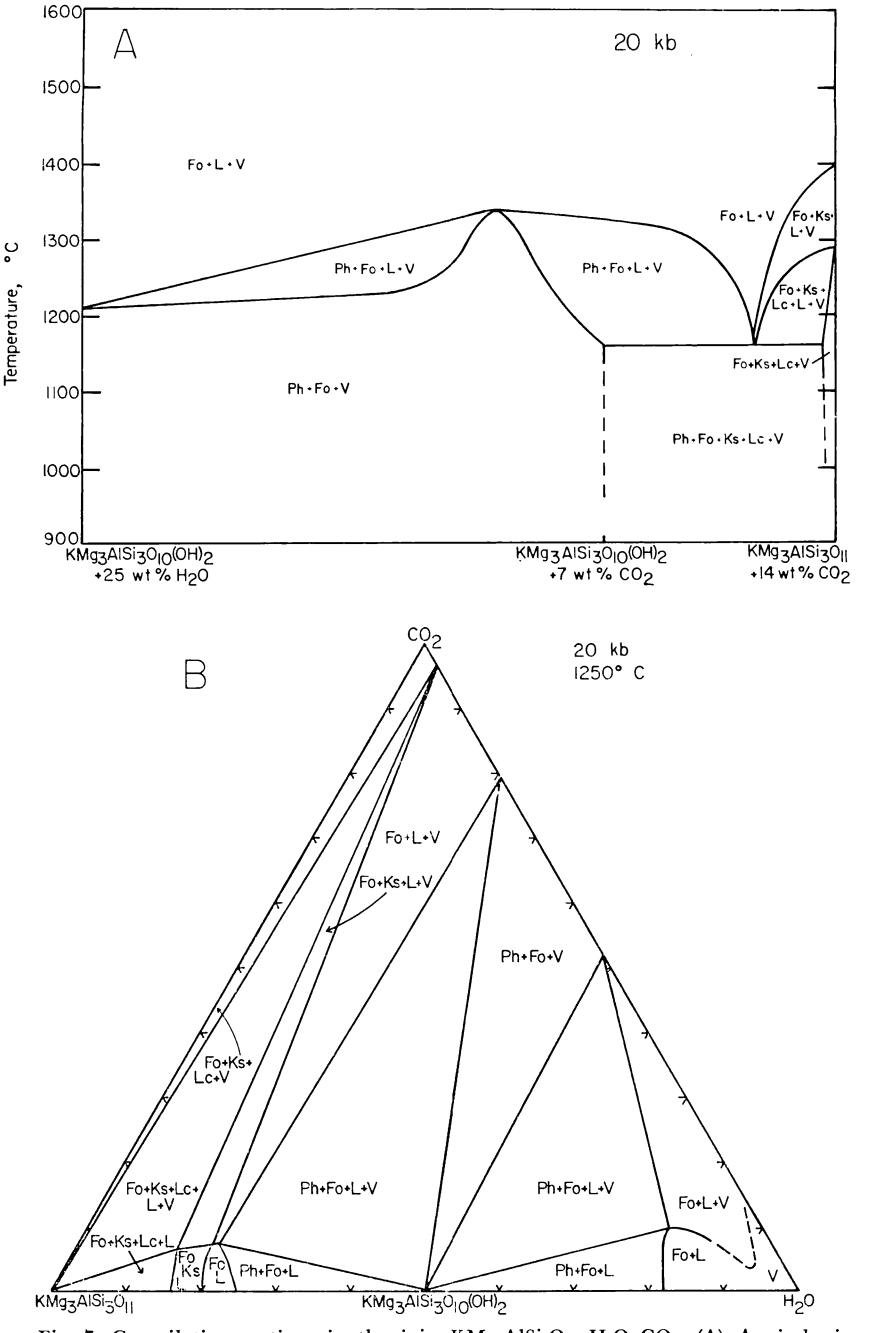

Fig. 7. Compilation sections in the join $KMg_3AlSi_3O_{11}$–H_2O–CO_2. (A) An isobaric section constructed from the data of figures 4, 5, and 6, illustrating the effect of CO_2 on the melting behavior of the two compositional regions defined in the text. The location of the join is given in figure 3. A trend of decreasing a_{H_2O} is defined from phlogopite + excess H_2O to anhydrous phlogopite + CO_2. Vapor compositions cannot be determined from this section. Abbreviations are the same as figure 4. (B) A schematic isobaric-isothermal section in the join $KMg_3AlSi_3O_{11}$–H_2O–CO_2 at 20 kb and 1250°C. Compositions are in mol percent and equilibrium vapor compositions are schematic. Abbreviations are the same as figure 4.

across the join $KMg_3AlSi_3O_{11}$–H_2O–CO_2 at 10 kb and 1225°C and observed that phlogopite stability in the region of relatively high a_{H_2O} was enhanced by CO_2. In figure 5, the results of additional quenching experiments involving phlogopite in the presence of excessive amounts of H_2O–CO_2 vapor are presented in a temperature-composition diagram. Vapor compositions at run conditions are unknown, because the proportion of subsolidus phlogopite is not constant, solubilities of H_2O and CO_2 are unknown, and phlogopite melts divariantly. Figure 5, therefore, is plotted as a function of the initial mol fraction of volatile constituents, excluding structural H_2O, added to the solid phases ($X_{CO_2}^{V_i}$).

The results of the current investigations are consistent with the observations of Yoder (1970) that with the addition of CO_2 to the assemblage phlogopite + H_2O (figs. 5 and 7A) phlogopite melts divariantly, and its maximum stability expands. At $X_{CO_2}^{V_i} = 0.64$, an azeotrope-like maximum occurs, and for more CO_2-rich compositions, the temperature of the phlogopite liquidus decreases. The geometric relation of the phases at this point is a planar arrangement of four phases satisfying the degenerate reaction

$$\text{phlogopite} + \text{vapor} \rightleftarrows \text{forsterite} + \text{liquid}. \quad (3)$$

The stability of phlogopite at this point is the same, within the limits of experimental precision, as the maximum stability of phlogopite in the absence of a vapor phase.

Stability maxima of amphiboles as a function of X_{CO_2} have been reported previously. Both Eggler (1972) and Holloway (1973) indicated that the maximum occurs as a result of decreasing H_2O content of the liquid with increasing $X_{CO_2}^{V}$, and that this maximum shifts to higher $X_{CO_2}^{V}$ with increasing pressure.

The divariant melting behavior of phlogopite (fig. 5) in the presence of large amounts of water-rich volatiles is similar to the melting behavior of mantle compositions as a function of excess H_2O–CO_2 vapor, inasmuch as solidus temperatures and liquid compositions vary as a continuous function of $X_{CO_2}^{V}$.

$KMg_3AlSi_3O_{10}(OH)_2$ + 7 percent CO_2–$KMg_3AlSi_3O_{11}$ + 7 percent CO_2.—The effect of CO_2 on phlogopite melting relations in the H_2O-deficient melting region is shown in figure 6. In figures 7A and 7B, the effects of CO_2 on phlogopite melting relations for the entire $KMg_3AlSi_3O_{11}$–H_2O–CO_2 join are summarized. As the a_{H_2O} decreases from the azeotrope-like point, the melting reaction changes character, becoming eutectic-like in appearance. Melting occurs at 1160° ± 12°C at 20 kb by the univariant reaction

$$\text{phlogopite} + \text{kalsilite} + \text{leucite} + \text{vapor} \rightleftarrows \text{forsterite} + \text{liquid}. \quad (4)$$

Because reaction (4) is univariant, the vapor composition is buffered, for a given pressure, at a unique value in a "zone of invariant vapor composition" (ZIVC) (Eggler, 1977). Another important feature of this reaction is that melting across a broad volatile composition range results in

a liquid of fixed composition. In figure 7B, it can be seen that this melting reaction determines phlogopite stability, when the total volatile content of the system is low. Melting behavior of this sort is in contrast to the melting of phlogopite in the presence of large quantities of volatiles.

Compositions with mol ratios of $KAlSiO_4/KAlSi_2O_6$ other than unity were not studied in this investigation nor that of Yoder and Kushiro (1969). Accordingly, only those phase fields cut by the join $KMg_3AlSi_3O_{10}(OH)_2$–$KMg_3AlSi_3O_{11}$–CO_2 are presented in the diagrams. The result is apparent in figures 4 and 6 where a four-phase field and a five-phase field, respectively, are conspicuously absent along portions of the solidus. The observed phase relation is kalsilite and leucite melting coincidentally at the solidus for these compositions. This melting behavior requires a singular relation at low pressures, where both kalsilite and leucite are simultaneous indifferent phases. Yoder and Kushiro (1969, p. 573-574) inferred the existence of such a point, on the vapor-absent univariant curve in the CO_2-absent system, at approx 2 kb and 1200°C. Alternatively, an undetected five-phase field, involving either kalsilite or leucite in addition to phlogopite + forsterite + liquid + vapor, may persist marginally above the solidus of figure 6 (and fig. 7A). The existence of this field requires two singular points, with kalsilite and leucite as separate indifferent phases, at low pressures. Because the five-phase field was not detected in these experiments, nor the four-phase field in those of Yoder and Kushiro (1969), and because the compositional limitation of the join investigated does not reveal the necessary information about the liquid composition, the phase relations are presented so as to be consistent with the existing data.

The Composition Join $KAlSiO_4$–Mg_2SiO_4–SiO_2–H_2O–CO_2

The orientation of reaction (4) in P–T space is illustrated in figure 8, which is a summary of some of the relevant experimentally-determined and geometrically-constrained relations in the system $KAlSiO_4$–MgO–SiO_2–H_2O–CO_2. The reaction originates at the CO_2-absent quaternary invariant point, I_{10} in figure 8, located at approx 1.5 kb and 1160°C (Yoder and Kushiro, 1969) and involving the phases phlogopite, forsterite, kalsilite, leucite, liquid, and vapor. The reaction was not bracketed at pressures below 20 kb, and its intersection with I_{10} is shown to be consistent with the melting reaction observed at high pressures.

Three additional univariant phlogopite melting reactions, for which the vapor compositions are buffered, occur for different bulk compositions than reaction (4) in the system $KAlSiO_4$–Mg_2SiO_4–SiO_2–H_2O–CO_2. These reactions,

$$\text{phlogopite} + \text{sanidine} + \text{vapor} \rightleftarrows \text{forsterite} + \text{leucite} + \text{liquid}, \quad (5)$$

$$\text{phlogopite} + \text{enstatite} + \text{sanidine} + \text{vapor} \rightleftarrows \text{forsterite} + \text{liquid}, \quad (6)$$

and

$$\text{phlogopite} + \text{sanidine} + \text{quartz} + \text{vapor} \rightleftarrows \text{enstatite} + \text{liquid}, \quad (7)$$

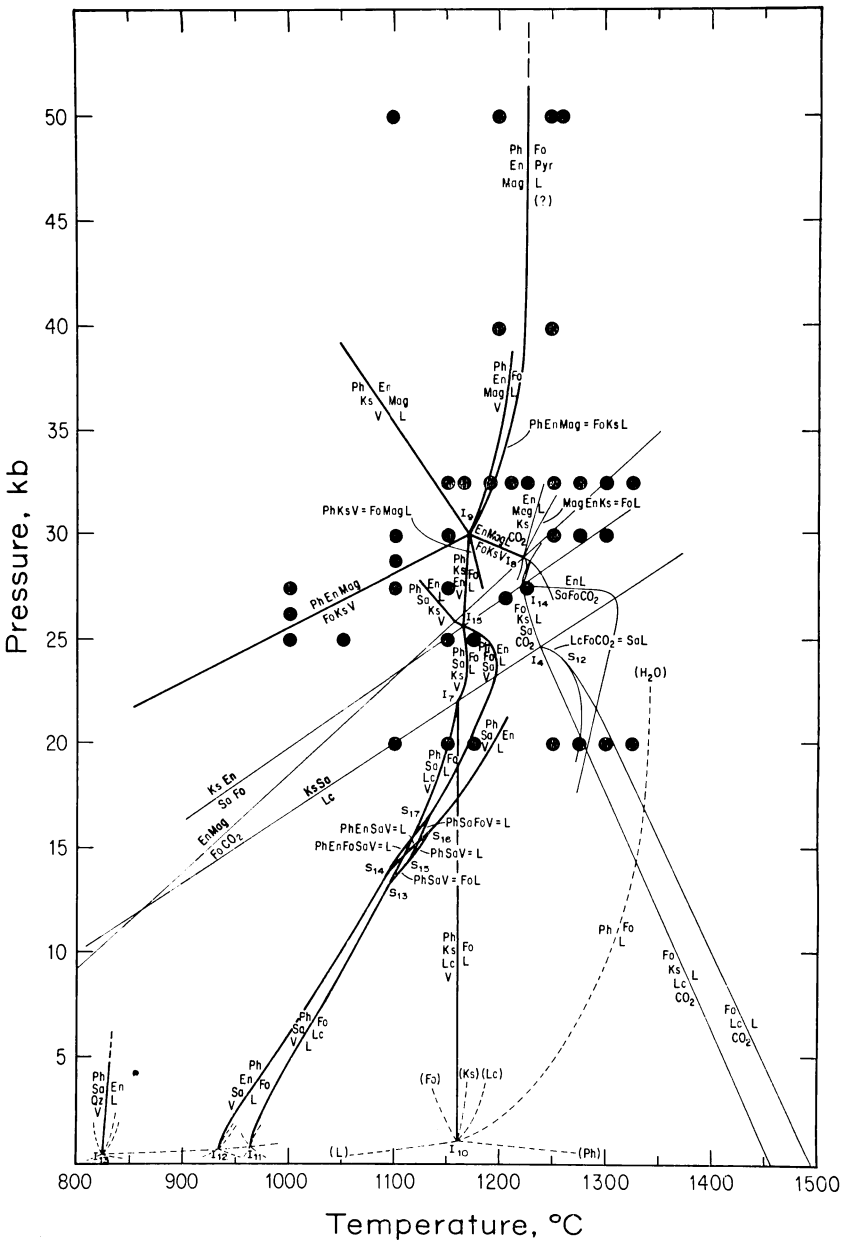

Fig. 8. P–T projection of phase relations involving phlogopite, enstatite, forsterite, magnesite, sanidine, kalsilite, leucite, liquid, and vapor in the system $KAlSiO_4$–MgO–SiO_2–H_2O–CO_2. Dashed lines at low pressure are reactions in the H_2O-saturated system (quaternary). The results for I_{10} are from Yoder and Kushiro (1969) and those for I_{11}, I_{12}, and I_{13} are from Luth (1967). Light solid lines are reactions in the CO_2-saturated system (quaternary) and volatile-absent subsolidus reactions that are discussed in part I of this paper. Heavy solid lines are univariant reactions in the H_2O–CO_2 system (quinary). The reaction leucite $\rightleftarrows$ sanidine + kalsilite is from Lindsley (1966) and the reaction enstatite + magnesite $\rightleftarrows$ forsterite + CO_2 is from Newton and Sharp (1975). Pyrope is observed as a reaction product at 40 kb and higher. Although kalsilite is a predicted reaction product at pressures above I_{10}, it was not observed in run products. Abbreviations are the same as figure 4, and additionally: En, enstatite; Mag, magnesite; Pyr, pyrope.

also emanate from low pressure invariant points (I_{11}, I_{12}, and I_{13}, respectively, in fig. 8) in the quaternary system $KAlSiO_4$–Mg_2SiO_4–SiO_2–H_2O (Luth, 1967). Reactions (5) and (6) occur for bulk compositions that model mantle peridotite: These reactions and others evolving from them at higher pressures and temperatures can be determined by Schreinemaker's methods, based on knowledge of end-member relations in the CO_2-absent system at low pressures (Luth, 1967), in the H_2O-absent system as a function of pressure and temperature (pt. 1), and in the quinary system at high pressures (this paper). When considered in conjunction with reaction (4) as a function of pressure, these reactions depict the evolution of the liquidus surface for the system $KAlSiO_4$–Mg_2SiO_4–SiO_2–H_2O–CO_2 and provide a basis for modelling the role of phlogopite in the genesis of potassium-rich magmas. Reaction (7) is not applicable to melting in the upper mantle because of its bulk composition and will not be considered in the following discussion. It represents, however, a minimum melting reaction in the quinary system (a possible endpoint for fractionation) and may be applicable to crustal anatexis.

The evolution of the liquidus surface for the system $KAlSiO_4$–Mg_2SiO_4–SiO_2–H_2O–CO_2 is comparable to that for the system $KAlSiO_4$–Mg_2SiO_4–SiO_2–CO_2 (pt. 1 of this paper); liquid compositions are quartz-normative at low pressures but become depleted in silica and enriched in potassium as the sanidine and enstatite primary phase fields expand with increasing pressure. Furthermore, the liquid compositions for reactions (5) and (6) cross over stable joins as the primary phase fields expand, in the same manner as did the liquids in equilibrium with model peridotite assemblages in the system $KAlSiO_4$–Mg_2SiO_4–SiO_2–CO_2. That is, reactions (5) and (6) cross in P–T projection without generating an invariant point. The systems differ, however, in that the presence of phlogopite introduces a new set of stable joins and thermal barriers.

At a pressure below 14 kb, sanidine ceases to melt incongruently; reaction (5) terminates at singular point S_{13} (fig. 8), and the new univariant melting reactions are

$$\text{phlogopite} + \text{sanidine} + \text{leucite} + \text{vapor} \rightleftarrows \text{forsterite} + \text{liquid} \quad (8)$$

and

$$\text{phlogopite} + \text{sanidine} + \text{vapor} \rightleftarrows \text{forsterite} + \text{liquid}. \quad (9)$$

At only slightly higher pressures, the liquid composition for the latter reactions must intersect the Ph–Sa–V join, generating S_{15} (forsterite is an indifferent phase) and creating Ph–Sa–V and Ph–Fo–Sa–V as thermal barriers by the reactions

$$\text{phlogopite} + \text{forsterite} + \text{sanidine} + \text{vapor} \rightleftarrows \text{liquid} \quad (10)$$

and

$$\text{phlogopite} + \text{sanidine} + \text{vapor} \rightleftarrows \text{liquid}. \quad (11)$$

The liquid composition for the other assemblage (reaction 6) is believed to intersect the Ph–Sa–En–V join at about 14 kb also (pt. 1), pro-

ducing singular point S_{14} (where forsterite is no longer a reaction product). At higher pressures, the liquid compositions for the reactions

$$\text{phlogopite} + \text{enstatite} + \text{forsterite} + \text{sanidine} + \text{vapor} \rightleftarrows \text{liquid} \quad (12)$$

and

$$\text{phlogopite} + \text{enstatite} + \text{sanidine} + \text{vapor} \rightleftarrows \text{liquid} \quad (13)$$

intersect the thermal barriers defined by the degenerate reactions (10) and (11) at singular points S_{16} and S_{17}. At still higher pressures, the predicted univariant reactions are

$$\text{phlogopite} + \text{forsterite} + \text{sanidine} + \text{vapor} \rightleftarrows \text{enstatite} + \text{liquid} \quad (14)$$

and

$$\text{phlogopite} + \text{sanidine} + \text{vapor} \rightleftarrows \text{enstatite} + \text{liquid}. \quad (15)$$

The relations described above coincide with the transition from quartz-normative to leucite-normative liquid compositions and are required in order to reconcile experimental observations of expanded enstatite and sanidine primary phase fields at higher pressures. Inasmuch as the liquid compositions are believed to be only slightly removed from the Ks–SiO_2 join to at least 20 kb (that is, small MgO and CO_2 solubilities in the liquids, and $P_{H_2O} << P_{total}$), the crossing of stable joins and temperature reversal are believed to occur over a slight pressure interval at about 14 kb. A similar pressure for the transition from simplified tholeiitic to alkalic basalts in the system CaO–MgO–Al_2O_3–SiO_2, 12 kb, has been proposed by Presnall and others (1978).

At approx 22 kb and 1160°C, there is an invariant point, I_7 (not directly investigated), involving five components and the phases phlogopite, forsterite, kalsilite, sanidine, leucite, liquid, and vapor. The postulated invariant point is generated by the intersection of reaction (4), reaction (8), and the subsolidus reaction

$$\text{kalsilite} + \text{sanidine} \rightleftarrows 2\ \text{leucite} \quad (16)$$

(Scarfe, Luth, and Tuttle, 1966; Lindsley, 1966). This point signifies the disappearance of the leucite stability field on the liquidus.

At pressures above 22 kb, the phlogopite melting reaction is

$$\text{phlogopite} + \text{kalsilite} + \text{sanidine} + \text{vapor} \rightleftarrows \text{forsterite} + \text{liquid}. \quad (17)$$

At approx 26 kb and 1170°C, this reaction intersects the subsolidus reaction

$$\text{sanidine} + 2\ \text{forsterite} \rightleftarrows \text{kalsilite} + 4\ \text{enstatite} \quad (18)$$

generating an invariant point, I_{15}. Also terminating at this point is reaction (14). At higher pressures, the Ks–En join replaces Sa–Fo as the stable join. The phase relations attending I_{15} are similar to those discussed for the H_2O-absent analog, I_{14} in the system $KAlSiO_4$–Mg_2SiO_4–SiO_2–CO_2, except that I_{15} is characterized by an additional component and is not

effectively portrayed in three dimensions. Reaction (18) is important with regard to the transition from silica-undersaturated liquids to extremely silica-undersaturated liquids (for example, carbonate-normative) with increasing pressure. At pressures above I_{15}, the phlogopite melting reaction is

$$\text{phlogopite} + \text{enstatite} + \text{kalsilite} + \text{vapor} \rightleftarrows \text{forsterite} + \text{liquid}. \quad (19)$$

Extrapolation of reaction (19) to higher pressures has resulted in the discovery of an invariant point (I_9 in fig. 8), at approx 30 kb and 1170°C, at which magnesite is introduced as a solidus phase. The existence of such a point has been postulated from theoretical considerations by Eggler and Holloway (1977). The point was located by the intersection of three univariant reactions: reaction (19), the devolatilization reaction

$$\text{phlogopite} + \text{enstatite} + \text{magnesite} \rightleftarrows \text{forsterite} + \text{kalsilite} + \text{vapor}, \quad (20)$$

and a melting reaction involving phlogopite + enstatite + magnesite as reactants that is discussed in detail later.

The phlogopite-absent reaction

$$\text{forsterite} + \text{kalsilite} + \text{vapor} \rightleftarrows \text{enstatite} + \text{magnesite} + \text{liquid} \quad (21)$$

emanates from I_9 tending toward higher temperatures and higher $X_{CO_2}^{V}$, and terminates at I_8, a H_2O-absent invariant point involving five components and the phases enstatite, forsterite, magnesite, kalsilite, sanidine, liquid, and vapor. This invariant point and other H_2O-absent phase relations in the system $KAlSiO_4$–Mg_2SiO_4–SiO_2–CO_2 are discussed elsewhere (pt. 1, p. 385-420).

At pressures above I_9, the vapor-absent reaction

$$\text{phlogopite} + \text{enstatite} + \text{magnesite} \rightleftarrows \text{forsterite} + \text{kalsilite} + \text{liquid} \quad (22)$$

involves two volatile-bearing minerals as solidus phases. Kalsilite was not observed as a reaction product, and it is inferred to persist only marginally above the solidus.

At slightly lower temperatures than reaction (22), the kalsilite-absent reaction

$$\text{phlogopite} + \text{enstatite} + \text{magnesite} + \text{vapor} \rightleftarrows \text{forsterite} + \text{liquid} \quad (23)$$

occurs for conditions of low total volatile contents in which there is sufficient H_2O to saturate the potential phlogopite. Reaction (23) is a ZIVC-type reaction; the vapor composition is buffered by reaction with the carbonate phase.

Also at pressures above I_9, the forsterite-absent melting reaction

$$\text{phlogopite} + \text{kalsilite} + \text{vapor} \rightleftarrows \text{enstatite} + \text{magnesite} + \text{liquid} \quad (24)$$

occurs for volatile contents characterized by insufficient H_2O to saturate the phlogopite but sufficient CO_2 to react out forsterite.

Reactions (23) and (24) were not investigated because of the uncertainties involved in generating the correct buffering conditions. Reaction (22), however, has been investigated to higher pressures. Because kalsilite does not persist above the solidus, the results for reaction (22) are applicable to reaction (23), except that the latter reactions will be displaced to lower temperatures.

The Composition Join $KMg_3AlSi_3O_{10}(OH)_2$–$MgSiO_3$–$MgCO_3$

Reactions involving the assemblage phlogopite + enstatite + magnesite have been investigated to pressures of 50 kb. The compositions and run data are shown in table 3, and the results are presented in P–T projection in figure 8. Pyrope is encountered as a product of reaction (22) at pressures of 40 kb and higher, suggesting that another invariant point occurs between 32.5 and 40 kb.

Temperature-composition sections have been investigated at 32.5, 40, and 50 kb along the composition join magnesite–(phlogopite/enstatite = 1) (wt ratio) in a reconnaissance fashion and are presented in figure 9, A, B, and C. The purpose of these runs was to bracket the solidus and to determine the relative position of the phlogopite and magnesite phase volumes at temperatures immediately above the solidus. The position of the eutectic-like point can be used to infer the composition of the liquid produced by the melting of phlogopite + enstatite + magnesite. These results are clearly a first approximation to a complicated series of sections and to the liquid compositions.

DISCUSSION OF EXPERIMENTAL RESULTS

Composition of the Vapor Phase

Recently, it has been theorized that vapor compositions at mantle conditions may be invariant, for a specified pressure and temperature, when volatile-bearing phases coexist with their breakdown products in a reaction relationship (Eggler, 1977, 1978b; Eggler and Holloway, 1977; Wyllie, 1977a,b). A buffered vapor composition is considered typical of mantle conditions; that is, volatiles are present in insufficient quantity to saturate the bulk composition in one or more volatile-bearing minerals. The important consequence of this observation is that solidus temperatures and melt compositions are restricted (Eggler, 1978b). An example of this principle has been found in the system $KAlSiO_4$–MgO–SiO_2–H_2O–CO_2, involving phlogopite and magnesite.

For pressures below the occurrence of carbonate as a solidus phase where the a_{H_2O} is sufficiently low that phlogopite coexists with its breakdown products at subsolidus conditions, the vapor composition is buf-

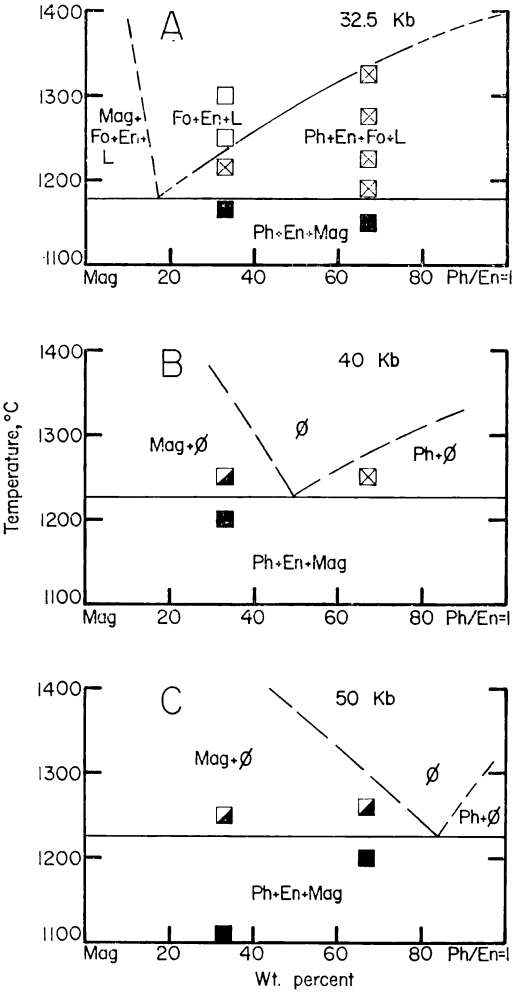

Fig. 9. Reconnaissance temperature-composition sections along the composition join magnesite–(phlogopite/enstatite=1) (wt ratio). (A) 32.5 kb; (B) 40 kb; (C) 50 kb. The symbol ϕ stands for the assemblage forsterite + pyrope + enstatite + liquid. Although the sections are more complicated than implied by the eutectic-like relationship between phlogopite and magnesite, the limited data do not allow elaboration. Abbreviations are the same as figure 8. Run symbols: Solid square, subsolidus; partially shaded square, magnesite melting interval; open square with cross, phlogopite melting interval; open square, neither phlogopite nor magnesite stable.

fered at a unique value for a given pressure and temperature as illustrated by reactions (4) to (15), (17), (19), and (24). The P–T coordinates for each reaction are defined by the intersection of the dehydration surface for the appropriate phlogopite-bearing assemblage as a function of $X_{CO_2}^{V}$ with the solidus surface for the divariant melting of this phlogopite-bearing assemblage as a function of $X_{CO_2}^{V}$. For the example investigated in detail at 20 kb, the composition $KMg_3AlSi_3O_{11}$–H_2O–CO_2, the phlogopite solidus surface is characterized by a thermal maximum at an intermediate $X_{CO_2}^{V}$ and approaches the dehydration surface from higher temperatures. The vapor composition associated with reaction (4) at this pressure is unique and will be buffered to higher H_2O contents with decreasing pressure and to higher CO_2 contents with increasing pressure. Similar variation in vapor compositions will be observed for all the reactions listed above.

The location of invariant point I_9 is uniquely defined in P–T–X_{CO_2} space by the intersection of three reaction surfaces: (1) the dehydration surface for phlogopite; (2) the solidus surface for phlogopite; and (3) the carbonation surface for the reaction

$$\text{enstatite} + \text{magnesite} \rightleftarrows \text{forsterite} + \text{vapor}. \qquad (25)$$

The divariant surfaces for the latter reaction have been contoured by Eggler, Kushiro, and Holloway (1976) at 26 kb as a function of $X_{CO_2}^{V}$, from which the vapor composition is estimated to be $X_{CO_2}^{V} = 0.6$ at I_9.

The univariant devolatilization reaction, (20), is defined by the intersection of the carbonation surface for reaction (25) with a phlogopite dehydration surface. Reaction (20) can be expressed in the general form

$$\text{phlogopite} + (1+X)\,\text{magnesite} + X\,\text{enstatite} \rightleftarrows$$
$$(2+X)\,\text{forsterite} + \text{kalsilite} + (1+X)\,CO_2 + H_2O. \qquad (20a)$$

The $X_{CO_2}^{V}$ defined by the reaction can vary; however, at any pressure, the temperature and vapor composition are fixed. At pressures below the reactions, either phlogopite or magnesite disappears, depending on their relative proportions and on the pressure; if the volatile portion of the bulk composition of the reactants is equal to $X_{CO_2}^{V}$ at the reaction boundary, both disappear.

For pressures in excess of I_9 (fig. 8), ZIVC-type solidi have been postulated for which the vapor composition is buffered by the carbonate phase (reaction 23) and by phlogopite (reaction 24). Reaction (23) is generated by the intersection of the magnesite carbonation surface with the solidus surface for the assemblage phlogopite + enstatite + magnesite. With increasing pressure, the vapor composition is buffered to higher H_2O–contents. Reaction (23) is of fundamental importance regarding the beginning of melting in the upper mantle for conditions at which sufficient H_2O exists to hydrate all potential phlogopite; if insufficient H_2O exists to hydrate all potential phlogopite, the vapor-absent reaction (22) defines the mantle solidus.

The forsterite-absent reaction (24) is the high-pressure extension of reaction (19). Vapor compositions are buffered to higher values of $X_{CO_2}^{V}$ with increasing pressure. The application of this reaction to partial melting in the upper mantle is extremely limited because excessive amounts of CO_2 (>20 wt percent) are necessary to carbonatize all the forsterite in typical peridotite compositions.

Liquid Compositions

Compositions of the liquids were not determined by electron microprobe in order to avoid uncertainties arising from the failure of carbonate-rich liquids and H_2O-rich liquids to quench unambiguously. Additionally, the liquid compositions applicable to magma generation are frequently those generated at or slightly above the solidus, where the volume of liquid is small. The approximate character of liquid compositions can be determined, however, from the phase relations and by reference to previous investigations.

Natural system.—In the absence of vapor, melt compositions are inferred to be similar to those observed by Kushiro and others (1972); small degrees of partial melting (several percent) between 20 to 30 kb will result in potassic, silica-undersaturated melts, perhaps analogous to leucite basanites or olivine leucitites. As indicated by Modreski and Boettcher (1973), the degree of silica-saturation varies from slightly quartz-normative at 10 kb to strongly leucite-normative at 30 kb. They inferred the congruent melting behavior of enstatite in the absence of a vapor (Boyd, England, and Davis, 1964) to be a principal determinant of the degree of silica-saturation. Larger degrees of partial melting, at temperatures above the phlogopite melting interval, will result in dilution of the alkaline nature of the melt, and melting relations will be controlled by the anhydrous melting behavior of lherzolite compositions (Kushiro, 1973); that is, the melts will assume a more tholeiitic and eventually picritic character.

For conditions of excess H_2O vapor and for the bulk composition studied, there is an interval of about 200°C between the lherzolite solidus and the phlogopite liquidus curve (fig. 2). Consequently, melt compositions will be initially controlled by the hydrous melting behavior of lherzolite (Mysen and Boettcher, 1975a,b). Only when the melting interval of phlogopite is encountered will substantial quantities of potassium enter the melt. Mysen and Boettcher (1975b) observed that the addition of 10 wt percent phlogopite to spinel lherzolite did not significantly increase the K_2O content of the liquid (K_2O <1.0 wt percent at 15 kb and 1025°C, for approx 20 percent liquid by volume) and suggested that high initial K_2O contents in the starting material did not necessarily imply that partial melts would be potassium-rich. The low potassium-content is reconciled by the observation that the melt composition they analyzed formed approx 100°C below the phlogopite liquidus and presumably below or only slightly into the phlogopite melting interval. Their melt composition is interesting, however, because it illustrates that

melt compositions below the phlogopite melting interval are extremely quartz-normative (31.9 percent quartz) and roughly analogous to andesitic liquids. These melt compositions reflect the incongruent melting of enstatite under water-saturated conditions (Kushiro, Yoder, and Nishikawa, 1968). When the phlogopite-component is released into the melt at a higher temperature, the chemical effect on the melt composition will be only slight (for moderate amounts of phlogopite in the starting material) because of the large volume of melt generated very rapidly at temperatures above the amphibole stability field (estimated by Mysen and Boettcher, 1975b, at more than 50 percent melt at 1200°C). These results are in agreement with the observations of Bravo and O'Hara (1975) that melting of hydrous phlogopite-bearing spinel or garnet lherzolite produces a melt with no obvious natural analogues.

Synthetic composition $KMg_3AlSi_3O_{11}$–H_2O–CO_2.—For conditions of high $a_{H_2O}^V$, phlogopite melts by reaction (3), and, clearly, the liquid composition must be potassium-rich and magnesium-poor. With the exception of the azeotrope-like point (fig. 7A), melting is divariant and characterized by solidus temperatures that vary as a function of $X_{CO_2}^V$. Furthermore, just as the partial melts from a peridotite source vary from silica-saturated to silica-undersaturated as a continuous function of $X_{CO_2}^V$ when there are large quantities of volatiles present (Mysen and Boettcher, 1975b; Eggler, 1973, 1975a), the contribution of phlogopite to these melt compositions will also vary as a function of $X_{CO_2}^V$.

For conditions of low $a_{H_2O}^V$, the phlogopite melting reaction occurring for this bulk composition is reaction (4). Inasmuch as all the phases are contained by the volume Ks–Lc–Fo–H_2O–CO_2, the liquid composition generated by reaction (4) is strongly silica-undersaturated and potassium-rich (kalsilite-normative) and is believed not to vary appreciably in the pressure interval to 22 kb. Because enstatite is not involved, reaction (4) is not a good model for partial melting of a mantle composition. Knowledge of reaction (4) is important, however, in understanding the evolution of the liquidus surface for the system $KAlSiO_4$–Mg_2SiO_4–SiO_2–H_2O–CO_2, and, in fact, at higher pressures than 22 kb, the enstatite primary phase field expands into the volume, and a high pressure derivative of reaction (4) (reaction 19) involves enstatite.

Synthetic system $KAlSiO_4$–Mg_2SiO_4–SiO_2–H_2O–CO_2.—In order to model effectively the role of phlogopite in magma genesis, the melting relations for a wide range of bulk compositions in the system $KAlSiO_4$–Mg_2SiO_4–SiO_2–H_2O–CO_2 must be understood. As mentioned above, there are four low pressure phlogopite-bearing assemblages in the system. Of these, one occurs for extremely silica-rich bulk compositions (Ph + Sa + En + Qz + L + V) and is not relevant to partial melting in the mantle. The second, Ph + Ks + Lc + Fo + L + V, has already been discussed and is of minor importance at pressures less than 22 kb, also as a result of compositional restrictions. The remaining two assemblages, Ph + Sa + Fo + Lc + L + V and Ph + En + Fo + Sa + L + V (reactions 5 and 6 at their origins, respectively), are important, because they model

mantle compositions and because their liquid compositions are sensitive to the principal features characterizing the phase relations in the system; that is, the expansion of the enstatite, sanidine, and phlogopite primary phase fields with increasing pressure.

As a consequence of these expanded stability regions a continuous range of liquid compositions can be derived that vary from quartz-normative at very low pressures to strongly kalsilite-normative at pressures approaching 30 kb. The particular reactions for assemblages containing enstatite and forsterite are shown in figure 10. Reactions (5) and (6) occur at low pressures and are characterized by liquids that are quartz-normative. At pressures somewhat below 14 kb, sanidine ceases to melt incongruently, the enstatite primary phase field expands beyond the Ph–En–Sa–V join, and liquids in equilibrium with Ph + Fo + En + Sa + V are forsterite-normative. At only slightly higher pressures, the enstatite primary phase field extends past the Ph–Fo–Sa–V join and liquids in equilibrium with Ph + Fo + En + Sa + V are leucite-normative. The enstatite field continues to expand with increasing pressure: liquids in equilibrium with Ph + Fo + En + Ks + V are strongly kalsilite-normative above 25 kb. Although details of the phase relations in this system and the H_2O-absent system differ, the major relations and the polybaric trend of melt compositions in equilibrium with peridotite minerals are closely comparable for both systems.

Synthetic join $KMg_3AlSi_3O_{10}(OH)_2$–$MgSiO_3$–$MgCO_3$.—As the pressure increases toward I_9, the solubility of CO_2 in liquid in equilibrium with Ph + Fo + En + Ks + V (reaction 19) must increase dramatically. This increase is required, because magnesite is stabilized as a solidus phase when reaction (19) intersects the devolatilization reaction (20). The phase relations at I_9 are analogous to those observed in the system CaO–MgO–SiO_2–CO_2 (Wyllie and Huang, 1975a, 1976; Eggler, 1975b) where intersection of the decarbonation reaction

$$\text{enstatite} + \text{dolomite} \rightleftarrows \text{forsterite} + \text{diopside} + \text{vapor} \qquad (26)$$

with the CO_2-saturated peridotite solidus results in stabilization of carbonate as a solidus phase and a change in liquid compositions to haplocarbonatites. In the present investigation, two volatile-bearing minerals and a buffered binary vapor phase are involved.

The compositions of phases occurring at I_9, notably magnesite and liquid, can no longer be defined by the components $KAlSiO_4$–Mg_2SiO_4–SiO_2–H_2O–CO_2 but, rather, are contained within the system $KAlSiO_4$–MgO–SiO_2–H_2O–CO_2. The compositions of melts produced at pressures in excess of I_9 by reactions (22) and (23) can be inferred from the isobaric sections presented in figure 9 at 32.5, 40, and 50 kb. When magnesite is initially introduced as a solidus phase, the composition of the melt is carbonate-rich and alkali-poor (fig. 9A). With increasing pressure the hypersolidus phlogopite stability field diminishes and that of magnesite expands. Accordingly, liquids become more potassic and silicic, suggesting a continuous trend between a predominantly carbonatitic melt at

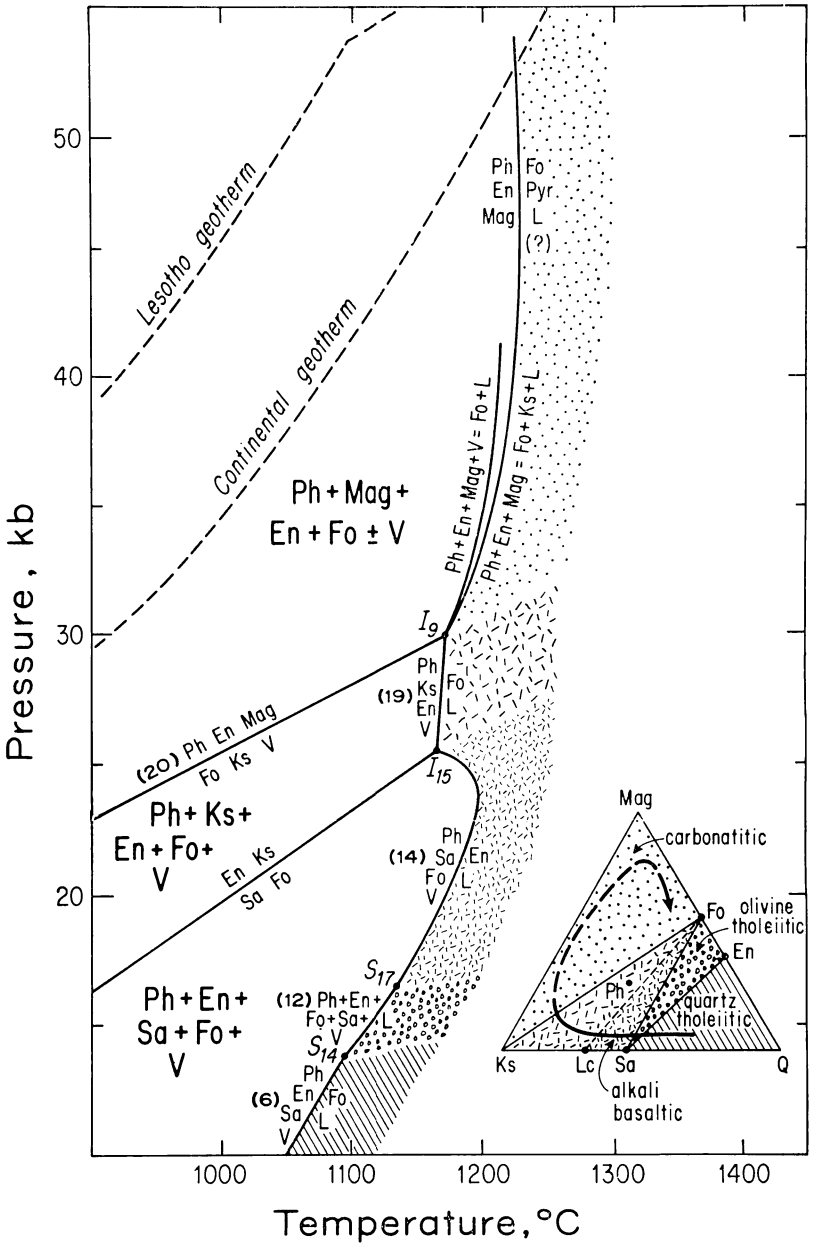

Fig. 10. Reactions in the system $KAlSiO_4$–MgO–SiO_2–H_2O–CO_2 that are applicable to the melting of assemblages containing forsterite and enstatite (peridotites). Numbers refer to reactions in the text. To the left of the solidus appear the assemblages that are stable when small amounts of volatiles are present. To the right of the solidus, patterns indicate the normative mineralogy of liquids produced by melting near the solidus; the normative liquids are keyed in the inset, a projection of liquids into the $KAlSiO_4$–MgO–SiO_2 base of the system. The heavy line shows the approximate trend of liquid compositions with increasing pressure. The compositions of alkali basaltic liquids are believed to change from leucite-normative to kalsilite-normative at about I_{15}. The continental geotherm is after Clark and Ringwood (1966); equilibrium pressures for the Lesotho geotherm were calculated by the "raw Al_2O_3" method (Boyd, 1973).

approx 30 kb and a more silicic and alkaline melt at higher pressures (fig. 9C).

GEOLOGIC APPLICATION

It is important to evaluate whether reactions that buffer the vapor composition are a realistic expectation in the upper mantle, and, if so, what the effects of these reactions are on the genesis of magmas.

Vapor Phase in the Mantle and Mantle Heterogeneity

The capacity of volatile-bearing minerals to be effective buffering agents of the vapor composition in the upper mantle is dependent on the bulk composition of the mantle system. The K_2O and H_2O contents of the upper mantle will determine the maximum possible amount of anhydrous phlogopite and the degree of saturation of the system in this potential phlogopite, respectively, whereas the CO_2 content will determine the degree of saturation of the system in carbonate component.

Estimates of the K_2O content of the mantle and whole Earth have been based on chrondritic abundances (Urey and Craig, 1953; Wasserburg and others, 1964), stony meteorite abundances (Brown, 1949), abundances of Rb and ^{40}Ar in the crust and atmosphere (Hurley, 1968a,b), heat generation requirements (Birch, 1951), concentrations in ultramafic rocks (Stueber and Murthy, 1966; Boyd and Nixon, 1973; Nixon and Boyd, 1973), empirical reconstructions of magma plus residual material in varying amounts (Ringwood, 1966), enrichment of K_2O in basalts (Kushiro, Syono, and Akimoto, 1967), and trace element fractionation models (Gast, 1968). According to these estimates, a K_2O content of the upper mantle of 0.15 wt percent is realistic. This content, however, corresponds to 1.3 wt percent potential phlogopite and requires only 0.06 wt percent H_2O to saturate. Estimates of H_2O content of the upper mantle are variable (Hess, 1962, 1964; Ringwood, 1966; Nicholls, 1967; Hurley, 1968b; Wyllie, 1971) but clearly in excess of this value and probably about 0.1 to 0.2 wt percent. An excess of water relative to potential phlogopite is therefore expected in an average upper mantle composition. However, there is no *a priori* reason to expect that the upper mantle is homogeneous (Hofmann and Hart, 1978), especially with regard to H_2O, CO_2, alkalies, Fe, Ti, LREE, et cetera. (Wyllie, 1979; Boettcher and O'Neil, 1980).

The buffering of vapor compositions by reactions with phlogopite, such as reactions (4), (8), (12), (14), (17), and (19), is best visualized in figure 7. Large total volatile contents (as in fig. 7A), equivalent to a section across figure 7B near the H_2O–CO_2 join, result in a zone of univariant melting behavior (a buffered region) that encompasses a reduced range of volatile compositions (remember that in the Ph + Ks + Fo + Lc + V region insufficient H_2O exists to saturate potential phlogopite). Small total volatile contents, equivalent to a section across figure 7B near the $KMg_3AlSi_3O_{11}$ apex, are typical of the upper mantle and will enlarge the region of univariant melting.

Because of the probable excess of water relative to potential phlogopite in "normal" upper mantle, phlogopite must be considered a weak buffer of vapor compositions. For these conditions and at pressures less than about 20 kb, the composition of a vapor will be more strongly buffered by amphibole (Eggler, 1978a), and, in fact, a portion of or all the available potassium may be incorporated in amphibole.

Phlogopite is believed to act as a buffer, on the other hand, in regions of the mantle that are heterogeneously enriched in potassium. The physico-chemical conditions that enhance the capacity of phlogopite to be a strong buffer of vapor compositions include pressures greater than amphibole stability limits, smaller volatile contents than estimated averages for the upper mantle, high proportions of K_2O in the source material, or a high proportion of CO_2 relative to H_2O. These conditions are similar to those proposed for the genesis of alkalic silica-undersaturated magmas, namely, small degrees of partial melting at moderate to high pressures of a material that is perhaps anomalously enriched in alkalies, LREE, Fe, Ti, and CO_2. It is believed that phlogopite can buffer the vapor composition in such cases at moderate to high pressures in the upper mantle, but that such cases are as occasional in occurrence as are potassium-rich silica-undersaturated magmas.

For conditions where carbonate can be a solidus phase, the vapor composition will be buffered by carbonate, by a reaction similar to (23). While the capacity of phlogopite to buffer the vapor is limited by the total volatile content and K_2O content of the system, there will never be sufficient CO_2 to saturate the potential carbonate in the upper mantle (>20 wt percent CO_2 is required). Consequently, carbonate has a large capacity to buffer the vapor composition, and melting in the mantle in the presence of a vapor will probably be initiated by a reaction analogous to (23). Solidus temperatures and melt compositions will be independent of the volatile composition and will vary principally as a function of the pressure of magma generation.

Metasomatism and Volatile Transport

The propensity for alkalies to be leached and transported by a fluid phase is evidenced by the occurrence of alkali metasomatic aureoles associated with alkaline complexes and, from an experimental point of view, by the vapor quench phases encountered during investigation of alkali-bearing systems. The frequent secondary textural appearances of phlogopite in many of the phlogopite-bearing nodules derived from the upper mantle (Dawson, 1962; Kushiro and Aoki, 1968; Smith, 1975; Boettcher and others, 1979) suggest the actions of alkali metasomatic processes in the upper mantle as well. Metasomatic introduction of phlogopite in the upper mantle may be a means of producing an anomalously phlogopite-enriched zone in an otherwise potassium-poor mantle and may be a precursor to alkali magma generation (Lloyd and Bailey, 1975). As Yoder (1976) and Kushiro and Aoki (1968) observed, this phlogopite-enrichment would necessitate an even deeper source for

the volatile fluid and solute components than the depth of origin of the magma, perhaps beyond the stability limit of phlogopite.

The results of this investigation suggest that vapor compositions, buffered at lower pressures by hydrous phases (usually amphibole but perhaps, rarely, phlogopite) and at higher pressures by carbonate, display compositional gradients as a function of pressure. A maximum value of $X_{CO_2}^V$ is attained at the onset of the carbonate stability region, becoming more H_2O-rich for both higher and lower pressures. Because the solute content of a vapor is greater for H_2O-rich fluids and increases with pressure (Burnham, 1967; Eggler and Rosenhauer, 1978), the effects of metasomatism will also increase with pressures in excess of 30 kb. The solute composition of a vapor, buffered by a carbonated and hydrated peridotite, is uniquely defined for a given pressure and temperature because the vapor composition is invariant at those conditions. It remains to determine that vapor composition as a function of pressure.

Magma Generation

The role of phlogopite in the genesis of potassic magmas, kimberlites, and carbonatites is primarily a function of total volatile content and pressure. For conditions where the vapor composition is buffered by reaction with phlogopite and at a pressure below the occurrence of carbonate as a solidus phase, the beginning of melting of a phlogopite peridotite is defined by the reactions shown on figure 10. Melt compositions vary continuously from quartz-normative at low pressures to kalsilite-normative at high pressures. Because phlogopite is not a strong buffer of vapor compositions, however, melting by these reactions would be the exception rather than the norm and would probably not occur at all below approx 20 kb except in mantle regions anomalously enriched in potassium. Amphibole, in contrast to phlogopite, will be a strong buffer of vapor compositions at these lower pressures because of the larger amount of amphibole that can be formed by hydrating a mantle peridotite composition (Mysen and Boettcher, 1975b). Although melting relations of amphibole peridotite in the presence of small quantities of volatiles will be similar in principle to those presented for phlogopite in this paper, the univariant melting reactions for amphibole-bearing assemblages and the liquid compositions produced by these reactions have yet to be determined. It is tempting to speculate that these melting relations may be applied to the genesis of volumetrically significant magma types, such as andesites, high-alumina basalts, and continental tholeiites.

Melting of phlogopite peridotite by reactions (14) and (19) may occur at pressures above 20 kb if the source material is H_2O-poor or K_2O- or CO_2-rich. For such conditions, small amounts of partial melt are expected. This melt would be leucite-normative at 20 kb and kalsilite-normative at higher pressures. The degree of silica-undersaturation is in concert with the observations of Mysen and Boettcher (1975b) for

partial melting of lherzolite for conditions of approximately $X_{CO_2}^{V} = 0.6$ and with analogous phase relations in $KAlSiO_4$–MgO–SiO_2–CO_2 (pt. 1).

The conditions necessary for phlogopite to buffer the vapor composition in the upper mantle are unusual, but not exceptional, and it is proposed that the relatively rare suite of highly potassic, silica-undersaturated magmas may have originated under these conditions. These rocks, which are comprised in large part by leucites, leucite tephrites, leucite nephelinites, nephelinites, and leucite basalts, are characterized by high K_2O and Al_2O_3 contents and low MgO and SiO_2 contents (pt. 1). Analogous melt compositions are predicted for partial melting of a phlogopite peridotite by reactions (14) and (19).

With increasing pressure, carbonate is introduced as a solidus phase. Relative to phlogopite, carbonate is a strong buffer of the vapor composition. The beginning of melting of carbonated mantle peridotite is determined by a reaction (analogous to 23) in which the vapor is buffered by a reaction with dolomite or magnesite (Kushiro, Satake, and Akimoto, 1975; Eggler, Kushiro, and Holloway, 1976) or, for vapor-absent conditions, by a reaction analogous to (22). (Holloway and Eggler, 1976, have also investigated the melting of a vapor-absent phlogopite–carbonate peridotite.) Small degrees of partial melting at lower pressures result in carbonatitic melts. With increasing pressure, the supersolidus stability of phlogopite decreases, and the principal melt component, derived from this breakdown of mica, becomes more silicic and potassic.

Eggler and Wendlandt (1979) have investigated the melting behavior of a kimberlite composition containing cobalt as a proxy for iron (Coons, Holloway, and Navrotsky, 1976) at 30 and 55 kb. A fundamental difference between the two isobars is the vastly enlarged supersolidus garnet stability volume at high pressures. At 30 kb, garnet disappears near the solidus, while at 55 kb, it persists approx 200°C above the solidus, and, along with olivine, clinopyroxene, and orthopyroxene, is in relatively close proximity to the liquidus. These observations and the phase relations on the phlogopite–enstatite–magnesite join support the contention that kimberlite can be produced by partial melting of a garnet lherzolite at the appropriate physical and volatile conditions, and that a continuous variation exists between carbonatitic melts at lower pressures and kimberlitic melts at higher pressures. Kimberlitic melts will be enriched in light rare earth elements relative to heavy rare earth elements, in concert with the observations of Haskin and others (1966), Mitchell and Brunfelt (1975), and Frey, Ferguson, and Chappell (1977).

The stability of phlogopite at pressures above 40 kb is probably pressure sensitive, and it is believed that at pressures in excess of 50 to 55 kb at approx 1200°C, phlogopite will cease to be a solidus phase. These conditions coincide with those for the maximum occurrence of phlogopite in nodules from kimberlite (Boyd and Nixon, 1975; Hearn and Boyd, 1975). Furthermore, the phlogopite + enstatite + magnesite solidus (fig. 10) intersects the continental (Clark and Ringwood, 1964) and Lesotho geotherms (Boyd, 1973) at approximately these conditions

(for vapor-present conditions these intersections will occur at slightly lower temperatures and pressures). It is proposed that for higher pressures defined by the mantle geotherm, phlogopite will not be stable, and traces of an intergranular liquid, rich in K_2O and H_2O, will exist. This region of incipient partial melting coincides with the provenance of both the discrete and sheared suites of nodules observed in kimberlites and is within the diamond stability field (Kennedy and Kennedy, 1976).

ACKNOWLEDGMENTS

Reviews of the manuscripts by Drs. A. L. Boettcher, D. M. Kerrick, B. O. Mysen, C. P. Thornton, E. B. Watson, and H. S. Yoder, Jr., are appreciated. The advice and pressure plate design of Dr. P. M. Bell facilitated the experiments at the high pressures. One of us (RFW) is grateful to Dr. H. S. Yoder, Jr., and the Geophysical Laboratory for the support received during a Predoctoral Fellowship. The research was supported in part by the National Science Foundation grants DES 73-00266AO1 and EAR 77-15704 to D. H. Eggler and EAR 73-00220AO2 to A. L. Boettcher.

REFERENCES

Bailey, D. K., 1970, Volatile flux, heat-focusing and the generation of magma, *in* Newall, G., and Rast, N., eds., Mechanism of Igneous Intrusion: Liverpool, Gallery Press, p. 177-186.

Birch, F., 1951, Recent work on the radioactivity of potassium and some related geophysical problems: Jour. Geophys. Research, v. 56, p. 107-126.

Boettcher, A. L., Mysen, B. O., and Allen, J. C., 1973, Techniques for the control of water fugacity and oxygen for experimentation in solid-media high-pressure apparatus: Jour. Geophys. Research, v. 78, p. 5898-5901.

Boettcher, A. L., and O'Neil, J. R., 1980, The origin of alkali basalts and kimberlites: Isotopic, chemical, and petrographic evidence: Am. Jour. Sci., v. 280-A, p. 594-621.

Boettcher, A. L., O'Neil, J. R., Windom, K. E., Stewart, D. C., and Wilshire, H. G., 1979, Metasomatism of the upper mantle and the genesis of kimberlites and alkali basalts, *in* Boyd, F. R., and Meyer, H. O. A., eds., The Mantle Sample: Inclusions in Kimberlite and Other Volcanics: Washington, D.C., Am Geophys. Union, p. 173-182.

Boettcher, A. L., and Wyllie, P. J., 1968, The calcite-aragonite transition measured in the system $CaO–CO_2–H_2O$: Jour. Geology, v. 76, p. 314-330.

Boyd, F. R., 1973, A pyroxene geotherm: Geochim. et Cosmochim. Acta, v. 37, p. 2533-2546.

Boyd, F. R., and England, J. L., 1960, Apparatus for phase-equilibrium measurements at pressures up to 50 kilobars and temperatures up to 1750°C: Jour. Geophys. Research, v. 65, p. 741-748.

Boyd, F. R., England, J. L., and Davis, B. T. C., 1964, Effects of pressure on the melting and polymorphism of enstatite, $MgSiO_3$: Jour. Geophys. Research, v. 69, p. 2101-2109.

Boyd, F. R., and Nixon, P. H., 1973, Structure of the upper mantle beneath Lesotho: Carnegie Inst. Washington Year Book 72, p. 431-445.

———— 1975, Origins of the ultramafic nodules from some kimberlites of northern Lesotho and the Monestery Mine, South Africa: Physics Chemistry Earth, v. 9, p. 431-454.

Bravo, M. S., and O'Hara, M. J., 1975, Partial melting of phlogopite-bearing synthetic spinel and garnet lherzolites: Physics Chemistry Earth, v. 9, p. 845-854.

Brown, H., 1949, A table of relative abundances of nuclear species: Rev. Modern Physics, v. 21, p. 625-634.

Burnham, C. W., 1967, Hydrothermal fluids at the magmatic stage, *in* Barnes, H. L., ed., Geochemistry of Hydrothermal Ore Deposits: New York, Holt, Rinehart, and Winston, Inc., p. 34-76.

Carswell, D. A., 1975, Primary and secondary phlogopites and clinopyroxenes in garnet lherzolite xenoliths: Physics Chemistry Earth, v. 9, p. 417-429.

Clark, S. P., Jr., and Ringwood, A. E., 1964, Density distribution and constitution of the mantle: Rev. Geophysics, v. 2, p. 35-88.

Coons, W. E., Holloway, J. R., and Navrotsky, A., 1976, Co^{2+} as a chemical analogue for Fe^{2+} in high temperature experiments in basaltic systems: Earth Planetary Sci. Letters, v. 30, p. 303-308.

Dawson, J. B., 1962, Basutoland kimberlites: Geol. Soc. America Bull., v. 73, p. 545-560.

Dawson, J. B., and Powell, D. G., 1969, Mica in the upper mantle: Contr. Mineralogy Petrology, v. 22, p. 223-237.

Dawson, J. B., and Smith, J. V., 1975, Chemistry and origin of phlogopite megacrysts in kimberlites: Nature, v. 253, p. 336-338.

Edgar, A. D., Green, D. H., and Hibberson, W. O., 1976, Experimental petrology of a highly potassic magma: Jour. Petrology, v. 17, p. 339-356.

Eggler, D. H., 1972, Amphibole stability in H_2O-undersaturated, calc–alkaline melts: Earth Planetary Sci. Letters, v. 15, p. 28-34.

———— 1973, Role of CO_2 in melting processes in the mantle: Carnegie Inst. Washington Year Book 72, p. 457-467.

———— 1974, Effect of CO_2 on the melting of peridotite: Carnegie Inst. Washington Year Book 73, p. 215-224.

———— 1975a, CO_2 as a volatile component of the mantle: the system Mg_2SiO_4–SiO_2–H_2O–CO_2: Physics Chemistry Earth, v. 9, p. 869-881.

———— 1975b, Peridotite–carbonate relations in the system CaO–MgO–SiO_2–CO_2: Carnegie Inst. Washington Year Book 74, p. 468-474.

———— 1976, Does CO_2 cause partial melting in the low-velocity layer of the mantle?: Geology, v. 4, p. 69-72.

———— 1977, The principle of the zone of invariant vapor composition: an example in the system CaO–MgO–SiO_2–H_2O and implications for the mantle solidus: Carnegie Inst. Washington Year Book 76, p. 428-435.

———— 1978a, Stability of dolomite in a hydrous mantle, with implications for the mantle solidus: Geology, v. 6, p. 397-400.

———— 1978b, The effect of CO_2 upon partial melting of peridotite in the system Na_2O–CaO–Al_2O_3–MgO–SiO_2–CO_2 to 35 kb, with an analysis of melting in a peridotite–H_2O–CO_2 system: Am. Jour. Sci., v. 278, p. 305-343.

Eggler, D. H., and Holloway, J. R., 1977, Partial melting of peridotite in the presence of H_2O and CO_2: principles and review, *in* Chapman Conference on Partial Melting in the Upper Mantle: Oregon Dept. Geology Mineral Ind. Bull., p. 15-36.

Eggler, D. H., Kushiro, I., and Holloway, J. R., 1976, Stability of carbonate minerals in a hydrous mantle: Carnegie Inst. Washington Year Book 75, p. 631-636.

Eggler, D. H., and Rosenhauer, M., 1978, Carbon dioxide in silicate melts: II. Solubilities of CO_2 and H_2O in $CaMgSi_2O_6$ (diopside) liquids and vapors at pressures to 40 kb: Am. Jour. Sci., v. 278, p. 64-94.

Eggler, D. H., and Wendlandt, R. F., 1979, Experimental studies on the relationship between kimberlite magmas and partial melting of peridotite, *in* Boyd, F. R., and Meyer, H. O. A., eds., Kimberlites, Diatremes, and Diamonds: Their Geology, Petrology, and Geochemistry: Washington, D.C., Am. Geophys. Union, p. 330-338.

Frey, F. A., Ferguson, J., and Chappell, B. W., 1977, Petrogenesis of South African and Australian kimberlite suites: Internat. Kimberlite Conf., 2d, Santa Fe, New Mexico, Extended Abs.

Gast, P. W., 1968, Trace element fractionation and the origin of tholeiitic and alkaline magma types: Geochim. et Cosmochim. Acta, v. 32, p. 1057-1086.

Hadidiacos, C., 1972, Temperature controller for high-pressure apparatus: Carnegie Inst. Washington Year Book 71, p. 620-622.

Haskin, L. A., Frey, F. A., Schmitt, R. A., and Smith, R. H., 1966, Meteoritic, solar and terrestrial rare-earth distributions: Physics Chemistry Earth, v. 7, p. 167-321.

Hearn, B. C., Jr., and Boyd, F. R., 1975, Garnet peridotite xenoliths in a Montana, U.S.A., kimberlite: Physics Chemistry Earth, v. 9, p. 247-255.

Hess, H. H., 1962, History of ocean basins, *in* Engel, A. E. J., James, H. L. and Leonard, B. F., eds., Petrologic Studies: A Volume to Honor A. F. Buddington: New York, Geol. Soc. America, p. 599-620.

———— 1964, The oceanic crust, the upper mantle and the Mayaguez serpentinized peridotite: Natl. Acad. Sci.-Natl. Research Council Pub. 1118, p. 169-175.

Hofmann, A. W., and Hart, S. R., 1978, An assessment of local and regional isotopic equilibrium in the mantle: Earth Planetary Sci. Letters, v. 38, p. 44-62.

Holloway, J. R., 1973, The system pargasite–H_2O–CO_2: a model for melting of a hydrous mineral with a mixed volatile fluid. I. Experimental results to 8 kb: Geochim. et Cosmochim. Acta, v. 37, p. 651-666.

Holloway, J. R., and Eggler, D. H., 1976, Fluid-absent melting of peridotite containing phlogopite and dolomite: Carnegie Inst. Washington Year Book 75, p. 636-639.

Hurley, P. M., 1968a, Absolute abundance and distribution of Rb, K and Sr in the Earth: Geochim. et Cosmochim. Acta, v. 32, p. 273-283.

———— 1968b, Correction to: Absolute abundance and distribution of Rb, K and Sr in the Earth: Geochim. et Cosmochim. Acta, v. 32, p. 1025-1030.

Jackson, E. D., and Wright, T. L., 1970, Xenoliths in the Honolulu volcanic series, Hawaii: Jour. Petrology, v. 11, p. 405-430.

Kennedy, C. S., and Kennedy, G. C., 1976, The equilibrium boundary between graphite and diamond: Jour. Geophys. Research, v. 81, p. 2467-2470.

Kushiro, I., 1973, Origin of some magmas in oceanic and circum-oceanic regions: Tectonophysics, v. 17, p. 211-222.

Kushiro, I., and Aoki, K. I., 1968, Origin of some eclogite inclusions in kimberlite: Am. Mineralogist, v. 53, p. 1347-1367.

Kushiro, I., Satake, H., and Akimoto, S., 1975, Carbonate–silicate reactions at high pressure and possible presence of dolomite and magnesite in the upper mantle: Earth Planetary Sci. Letters, v. 28, p. 116-120.

Kushiro, I., Shimizu, N., Nakamura, Y., and Akimoto, S., 1972, Compositions of coexisting liquid and solid phases formed upon melting of natural garnet and spinel lherzolites at high pressures: a preliminary report: Earth Planetary Sci. Letters, v. 14, p. 19-25.

Kushiro, I., Syono, Y., and Akimoto, S., 1967, Stability of phlogopite at high pressures and possible presence of phlogopite in the Earth's upper mantle: Earth Planetary Sci. Letters, v. 3, p. 197-203.

Kushiro, I., Yoder, H. S., Jr., and Nishikawa, M., 1968, Effect of water on the melting of enstatite: Geol. Soc. America Bull., v. 19, p. 1685-1692.

Lindsley, D. H., 1966, P–T projection for part of the system kalsilite–silica: Carnegie Inst. Washington Year Book 65, p. 244-247.

Lloyd, F. E., and Bailey, D. K., 1975, Light element metasomatism of the continental mantle: the evidence and the consequences: Physics Chemistry Earth, v. 9, p. 389-416.

Luth, W. C., 1967, Studies in the system $KAlSiO_4$–Mg_2SiO_4–SiO_2–H_2O: I. Inferred phase relations and petrologic applications: Jour. Petrology, v. 8, p. 372-416.

Luth, W. C., and Ingamells, C. O., 1965, Gel preparation of starting materials for hydrothermal experimentation: Am. Mineralogist, v. 50, p. 255-258.

Markov, V. K., Petrov, V. P., Delitsin, I. S., and Ryabinin, Y., 1966, Phlogopite transformations at high pressures and temperatures: Geochemistry Internat., v. 2, p. 1112-1120.

Mitchell, R. H., and Brunfelt, A. O., 1975, Rare earth element geochemistry of kimberlite: Physics Chemistry Earth, v. 9, p. 671-686.

Modreski, P. J., and Boettcher, A. L., 1972, The stability of phlogopite and enstatite at high pressures: a model for micas in the interior of the Earth: Am. Jour. Sci., v. 272, p. 852-869.

———— 1973, Phase relationships of phlogopite in the system K_2O–MgO–CaO–Al_2O_3–SiO_2–H_2O to 35 kilobars: a better model for micas in the interior of the Earth: Am. Jour. Sci., v. 273, p. 385-414.

Mysen, B. O., and Boettcher, A. L., 1975a, Melting of a hydrous mantle: I. Phase relations of natural peridotite at high pressures and temperatures with controlled activities of water, carbon dioxide and hydrogen: Jour. Petrology, v. 16, p. 520-548.

———— 1975b, Melting of a hydrous mantle: II. Geochemistry of crystals formed by anatexis of mantle peridotite at high pressures and high temperatures as a function of controlled activities of water, hydrogen and carbon dioxide: Jour. Petrology, v. 16, p. 549-593.

Newton, R. C., and Sharp, W. E., 1975, Stability of forsterite + CO_2 and its bearing on the role of CO_2 in the mantle: Earth Planetary Sci. Letters, v. 26, p. 239-244.

Nicholls, G. D., 1967, Geochemical studies in the ocean as evidence for the composition of the mantle, *in* Runcorn, S. K., ed., Mantles of the Earth and Terrestrial Planets: London, Intersci. Publishers, p. 285-304.

Nixon, P. H., and Boyd, F. R., 1973, Petrogenesis of the granular and sheared ultrabasic nodule suite in kimberlites, *in* Nixon, P. H., ed., Lesotho Kimberlites: Maseru, Lesotho, Lesotho Devel. Corp., p. 48-56.

Presnall, D. C., Dixon, S. A., Dixon, J. R., O'Donnell, T. H., Brenner, N. L., Schrock, R. L., and Dycus, D. W., 1978, Liquidus phase relations on the join diopside–forsterite–anorthite from 1 atm to 20 kbar: Their bearing on the generation and crystallization of basaltic magma: Contr. Mineralogy Petrology, v. 66, p. 203-220.

Ringwood, A. E., 1966, The chemical composition and origin of the Earth, *in* Hurley, P. M., ed., Advances in Earth Science: Cambridge, Mass., M.I.T. Press, p. 287-356.

Scarfe, C. M., Luth, W. C., and Tuttle, O. F., 1966, An experimental study bearing on the absence of leucite in plutonic rocks: Am. Mineralogist, v. 51, p. 726-735.

Smith, J. V., 1975, Chemistry of Mg-rich micas from kimberlites and xenoliths, with implications for volatiles in the upper mantle: Geol. Soc. America Abs. with Programs, v. 7, p. 1275-1276.

Stueber, A. M., and Murthy, V. R., 1966, Potassium:ribidium ratio in ultramafic rocks: differentiation history of the upper mantle: Science, v. 153, p. 740-741.

Urey, H. C., and Craig, H., 1953, The composition of the stone meteorites and the origin of the meteorites: Geochim. et Cosmochim. Acta, v. 4, p. 36-82.

Wasserburg, G. J., MacDonald, G. J. F., Hoyle, F., and Fowler, W. A., 1964, Relative contributions of uranium, thorium, and potassium to heat production in the Earth: Science, v. 143, p. 465-467.

White, R. W., 1966, Ultramafic inclusions in basaltic rocks from Hawaii: Contr. Mineralogy Petrology, v. 12, p. 245-314.

Wyllie, P. J., 1971, Role of water in magma generation and initiation of diapiric uprise in the mantle: Jour. Geophys. Research, v. 76, p. 1328-1338.

———— 1977a, Peridotite–H_2O–CO_2, and carbonatitic liquids in the upper asthenosphere: Nature, v. 266, p. 45-47.

———— 1977b, Mantle fluid composition buffered by carbonates in peridotite–CO_2–H_2O: Jour. Geology, v. 85, p. 187-207.

———— 1979, Kimberlite magmas from the system peridotite–CO_2–H_2O, *in* Boyd, F. R., and Meyer, H. O. A., eds., Kimberlites, Diatremes, and Diamonds: Their Geology, Petrology, and Geochemistry: Washington, D.C., Am. Geophys Union, p. 319-329.

Wyllie, P. J., and Huang, W. L., 1975a, Influence of mantle CO_2 in the generation of carbonatites and kimberlites: Nature, v. 257, p. 297-299.

———— 1975b, Peridotite, kimberlite, and carbonatite explained in the system CaO–MgO–SiO_2–CO_2: Geology, v. 3, p. 621-624.

———— 1976, Carbonation and melting reactions in the system CaO–MgO–SiO_2–CO_2 at mantle pressures with geophysical and petrological applications: Contr. Mineralogy Petrology, v. 54, p. 79-107.

Wyllie, P. J., and Tuttle, O. F., 1960, The system CaO–CO_2–H_2O and the origin of carbonatites: Jour. Petrology, v. 1, p. 1-46.

Yoder, H. S., Jr., 1970, Phlogopite–H_2O–CO_2: an example of the multicomponent gas problem: Carnegie Inst. Washington Year Book 68, p. 236-240.

———— 1976, Generation of Basaltic Magma: Washington, D.C., Natl. Acad. Sci., 265 p.

Yoder, H. S., Jr., and Eugster, H. P., 1954, Phlogopite synthesis and stability range: Geochim. et Cosmochim. Acta, v. 6, p. 157-185.

Yoder, H. S., Jr., and Kushiro, I., 1969, Melting of a hydrous phase: phlogopite: Am. Jour. Sci., v. 267-A (Schairer v.), p. 558-582.